

## Defining the Mechanism of Action and Enzymatic Selectivity of Psammaplin A against Its Epigenetic Targets

Matthias G. J. Baud,<sup>†</sup> Thomas Leiser,<sup>‡</sup> Patricia Haus,<sup>‡</sup> Sharon Samlal,<sup>§</sup> Ai Ching Wong,<sup>§</sup> Robert J. Wood,<sup>§</sup> Vanessa Petrucci,<sup>#</sup> Mekala Gunaratnam,<sup>#</sup> Siobhan M. Hughes,<sup>⊥</sup> Lakjaya Buluwela,<sup>⊥</sup> Fabrice Turlais,<sup>§</sup> Stephen Neidle,<sup>#</sup> Franz-Josef Meyer-Almes,<sup>‡</sup> Andrew J. P. White,<sup>†</sup> and Matthew J. Fuchter<sup>\*†</sup>

<sup>†</sup>Department of Chemistry, Imperial College London, London SW7 2AZ, United Kingdom

<sup>‡</sup>Department of Chemical Engineering and Biotechnology, University of Applied Sciences, Schnittspahnstrasse 12, 64287 Darmstadt, Germany

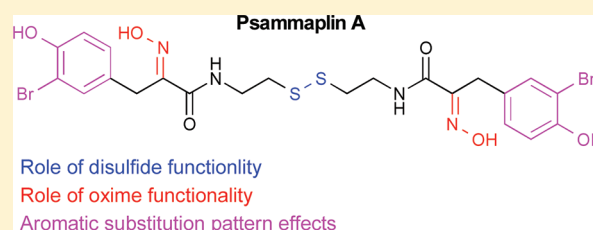
<sup>§</sup>Cancer Research Technology Discovery Laboratories, Wolfson Institute for Biomedical Research, The Cruciform Building, Gower Street, London WC1E 6BT, United Kingdom

<sup>#</sup>Cancer Research UK Biomolecular Structure Group, The School of Pharmacy, University of London, 29-39 Brunswick Square, London WC1N 1AX, United Kingdom

<sup>⊥</sup>Department of Surgery and Cancer, Imperial College London, Du Cane Road, London W12 0NN, United Kingdom

### **S** Supporting Information

**ABSTRACT:** Psammaplin A (**11c**) is a marine metabolite previously reported to be a potent inhibitor of two classes of epigenetic enzymes: histone deacetylases and DNA methyltransferases. The design and synthesis of a focused library based on the psammaplin A core has been carried out to probe the molecular features of this molecule responsible for its activity. By direct in vitro assay of the free thiol generated upon reduction of the dimeric psammaplin scaffold, we have unambiguously demonstrated that **11c** functions as a natural prodrug, with the reduced form being highly potent against HDAC1 in vitro (IC<sub>50</sub> 0.9 nM). Furthermore, we have shown it to have high isoform selectivity, being 360-fold selective for HDAC1 over HDAC6 and more than 1000-fold less potent against HDAC7 and HDAC8. SAR around our focused library revealed a number of features, most notably the oxime functionality to be important to this selectivity. Many of the compounds show significant cytotoxicity in A549, MCF7, and W138 cells, with the SAR of cytotoxicity correlating to HDAC inhibition. Furthermore, compound treatment causes upregulation of histone acetylation but little effect on tubulin acetylation. Finally, we have found no evidence for **11c** functioning as a DNMT inhibitor.



### ■ INTRODUCTION

Mechanisms of oncogenesis via the covalent modification of chromatin are becoming increasingly apparent. Such epigenetic control of chromatin organization directly affects gene expression and is a common molecular mechanism by which genes involved in the regulation of cell differentiation, proliferation, and survival are misregulated in cancer. Clearly, small molecule inhibitors of epigenetic pathways could be of use not only as leads for anticancer therapeutics but also as selective probes to study the interplay between epigenetic events and gene expression and how such events are aberrant in cancer.

Two of the most commonly studied epigenetic phenomena are DNA methylation and acetylation/deacetylation of the histone tails that protrude from the nucleosome. DNA can be methylated at the C5 position of cytosine, predominantly within the CpG dinucleotide, by the DNA methyltransferase family of enzymes (DNMTs), which use S-adenosyl methionine (SAM) as a cofactor. The so-called CpG islands are located in the promoter regions of approximately 50% of genes, and

hypermethylation generally results in gene silencing via the prevention of transcription factor binding<sup>1</sup> or the recruitment of multiprotein transcriptional repressor complexes. Currently, there are five known human DNMTs: DNMT1, -2, -3a, -3b, -3L, all of which have catalytic function except for DNMT2<sup>2,3</sup> and DNMT3L, which lack the amino-terminal regulatory domain and the catalytic domain, respectively. While DNMT1 preferentially methylates hemimethylated DNA and has been implicated in regulatory methylation for cellular maintenance, DNMT3a and -3b are known as de novo methylases, able to methylate previously unmethylated DNA and notably responsible for the establishment of DNA methylation patterns during embryogenesis.<sup>4</sup> Although devoid of a catalytic domain, DNMT3L has been found to interact with de novo DNMTs.<sup>5–10</sup>

Acetylation/deacetylation of the lysine residues on histone tails is mediated by the histone acetyltransferases (HATs) and

Received: November 29, 2011

Published: January 26, 2012

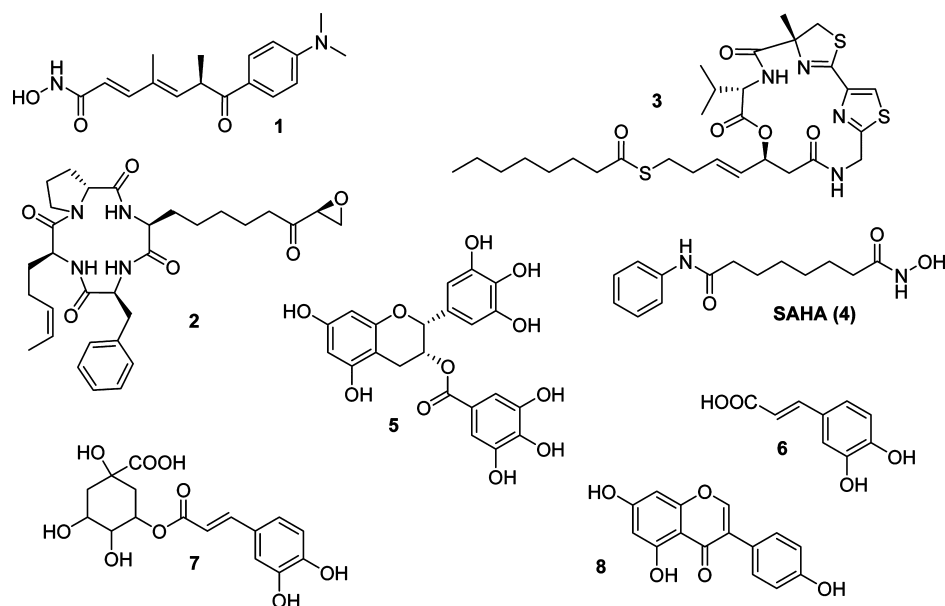


**Figure 1.** Examples of HDAC and DNMT inhibitors.

histone deacetylases (HDACs), respectively. HDACs mediate transcriptional repression through chromatin condensation. So far, 18 human genes that encode proven or putative HDACs have been identified, which can be divided into two categories, the zinc-dependent enzymes (classes I, II, and IV) and the  $\text{NAD}^+$ -dependent enzymes (class III, SirT1–7).<sup>4</sup> Class I HDACs are mostly expressed in the nucleus and include HDAC1, -2, -3, and -8. Class II HDACs are larger than class I enzymes and are tissue specific, shuttling between the cytoplasm and nucleus.<sup>11–13</sup> Indeed, certain HDACs have been shown to be able to deacetylate nonhistone proteins, such as hormone receptors, chaperone proteins, transcription factors, and cytoskeletal proteins.<sup>13,14</sup> Class II is further subdivided into class IIa (HDAC4, -5, -7, and -9) and class IIb (HDAC6 and -10) according to their sequence homology, structural characteristics, and number of catalytic domains. The recently identified HDAC11 constitutes its own class IV. Class III HDACs, also known as the sirtuins, are structurally and mechanistically distinct proteins.

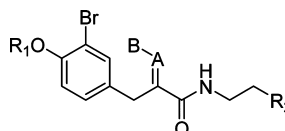
Natural products continue to play a significant role in anticancer drug discovery. A number of HDAC inhibitors isolated from natural sources have been reported,<sup>4,15,16</sup> including for example trichostatin A (1), trapoxin B (2), and largazole (3) (Figure 1). The synthetic compound suberoylanilide hydroxamic acid (SAHA) (4) was the first HDAC inhibitor approved by the FDA for the treatment of cancer and is used against cutaneous T-cell lymphomas.<sup>17,18</sup> Naturally occurring DNMT inhibitors have also been reported, specifically polyphenols such as EGCG (5),<sup>19</sup> caffeic acid (6), chlorogenic acid (7),<sup>20</sup> and genistein (8).<sup>21</sup> Psammappin A (11c, see Table 1) is a member of a family of natural products isolated from several marine sponges including *Pseudoceratina purpurea*.<sup>22</sup> It was characterized in 1987<sup>23–25</sup> and represents the first example of a natural product containing disulfide and oxime moieties isolated from a marine sponge. While 11c has been implicated as an inhibitor of numerous targets such as topoisomerase II,<sup>26</sup> DNA gyrase,<sup>27</sup> leucine aminopeptidase,<sup>28</sup> farnesyl protein transferase,<sup>28</sup> chitinase,<sup>29</sup> mycothiol-S-conjugate amidase,<sup>30</sup> aminopeptidase N,<sup>31</sup> and DNA polymerase  $\alpha$ -primase,<sup>32</sup> studies by Crews and co-workers showed it to be an

extremely potent inhibitor of both HDAC and DNMT enzymes.<sup>22</sup> In enzyme-based assays, 11c displayed potent activity ( $\text{IC}_{50}$ ) against an HDAC cell extract (4.2 nM) and semipurified DNMT1 (18.6 nM). Subsequently, studies on the antiproliferative properties of 11c in vitro have shown it to have significant cytotoxicity ( $\text{ED}_{50}$ ,  $\mu\text{g}/\text{mL}$ ) against human lung (A549, 0.57), ovarian (SK-OV-3, 0.14), skin (SK-MEL-2, 0.13), CNS (XF498, 0.57), and colon (HCT15, 0.68) cancer cell lines.<sup>33a</sup> In vivo, it inhibited tumor growth in the A549 lung xenograph mouse model while maintaining low toxicity.<sup>22</sup> Recently, the anticancer properties of psammappin A analogues have been explored en route to novel anticancer drugs.<sup>33b</sup>

In the present study, we report on the synthesis and biological evaluation of a library of psammappin A analogues to determine the chemical features necessary for HDAC and DNMT activity. In particular we wished to (1) unambiguously determine whether 11c functions as a natural prodrug for HDACs,<sup>34,35</sup> (2) determine the HDAC isoform selectivity of the natural product and our analogues, (3) investigate the reported DNMT activity using a functional DNMT1 assay, and (4) investigate the cellular effects of our compounds. At the outset, we envisaged that such study would not only allow dissection of the epigenetic activity of 11c but would also inform on new design motifs for the discovery of novel epigenetic inhibitors. Indeed, non-nucleoside DNMT inhibitors and isoform-selective HDAC inhibitors are severely underdeveloped, vindicating the need for new small molecules in these areas. Furthermore, epigenetic pathways such as histone deacetylation and DNA methylation are intimately interrelated, with the efficacy of HDAC inhibitors potentiated by coadministration of DNMT inhibitors in certain cases. Clearly, inhibitory molecules with dual activity against several classes of epigenetic enzymes may provide new approaches to epigenetic therapy.

## RESULTS

**Library Synthesis.** To establish SAR for 11c around our targets of interest, we designed and synthesized a library of compounds. The library was designed to probe the nature of the sulfur end group (disulfide, thioether, thiol, etc.) and the

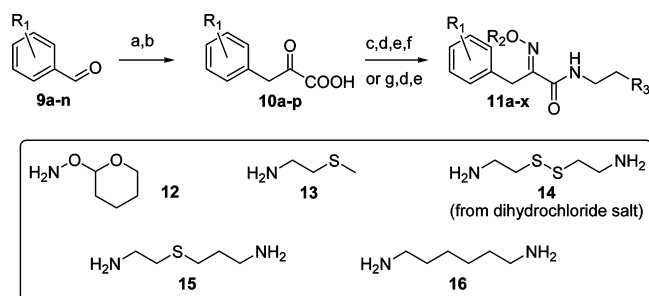
Table 1. HDAC Inhibition Data<sup>a</sup>


compd	R <sub>1</sub>	AB	R <sub>2</sub> <sup>b</sup>	rHDAC1 IC <sub>50</sub> [μM]	rHDAC6 IC <sub>50</sub> [μM]	IC <sub>50</sub> <sup>6/1 c</sup>
11a	H	NOH	SMe	7.7	>50	
11b	Me	NOH	SMe	23.3	>50	
11c	H	NOH	S <sub>2</sub> R (dimer)	0.045	2.8	62
11d	Me	NOH	S <sub>2</sub> R (dimer)	0.043	2.0	47
11c'	H	NOH	SH	0.0009	0.36	400
11d'	Me	NOH	SH	0.0018	3.2	1778
11e	H	NOMe	SMe	11.0	>50	
11f	Me	NOMe	SMe	>50	>50	
11g	H	NOMe	S <sub>2</sub> R (dimer)	0.38	9.5	25
11h	Me	NOMe	S <sub>2</sub> R (dimer)	0.22	>50	>227
11g'	H	NOMe	SH	0.027	0.22	8.1
11h'	Me	NOMe	SH	0.015	2.7	180
17a	H	O	SMe	7.3	ca. 30	
17b	Me	O	SMe	>50	>50	
17c	H	O	S <sub>2</sub> R (dimer)	5	9	1.8
17d	Me	O	S <sub>2</sub> R (dimer)	9	8	0.9
17c'	H	O	SH	0.40	1.0	2.5
17d'	Me	O	SH	1.1	0.25	0.23
18a	H	NNH <sub>2</sub>	SMe	ca. 50	>50	
18b	Me	NNH <sub>2</sub>	SMe	12.6	>50	
18c	H	NNH <sub>2</sub>	S <sub>2</sub> R (dimer)	6.1	5	0.8
18d	Me	NNH <sub>2</sub>	S <sub>2</sub> R (dimer)	3	>50	>16
18c'	H	NNH <sub>2</sub>	SH	0.005	1.0	200
18d'	Me	NNH <sub>2</sub>	SH	0.006	0.32	53
23	H	H <sub>2</sub>	S <sub>2</sub> R (dimer)	>50	20.2	<0.4
23'	H	H <sub>2</sub>	SH	0.42	1.1	2.6
24	H	NOH	C(O)NHOH	0.002	0.19	95
25	H	NOH	CH <sub>2</sub> C(O)NHOH	0.31	1.7	5.5
4				0.030	0.21	7
TCEP				>25	>25	

<sup>a</sup>IC<sub>50</sub> values for 11c and synthetic analogues against HDAC1 and HDAC6. <sup>b</sup>Thiols were prepared by in situ reduction of the respective disulfides using tris(2-carboxyethyl)phosphine hydrochloride (TCEP) and used immediately (see Experimental Section for details). <sup>c</sup>IC<sub>50</sub><sup>6/1</sup> is defined by the ratio IC<sub>50</sub><sup>HDAC6</sup>/IC<sub>50</sub><sup>HDAC1</sup>.

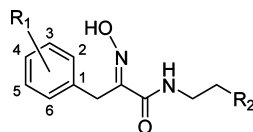
oxime functionality and to fully explore variation in the substituents of the aromatic “capping” group.

We have recently reported the synthesis of psammaplin A analogues bearing an oxime or *O*-methyloxime (see Scheme 1)

Scheme 1. <sup>a</sup>

<sup>a</sup>Reagents and conditions: (a) NaOAc, *N*-Ac-Gly, Ac<sub>2</sub>O, reflux; (b) 10% aq HCl, reflux; (c) 12, pyridine, rt; (d) EDCl, NHS, dioxane, rt; (e) 13 or 14 or 15<sup>65</sup> or 16, NEt<sub>3</sub>, dioxane/MeOH, rt; (f) HCl, CH<sub>2</sub>Cl<sub>2</sub>/Et<sub>2</sub>O/MeOH, reflux; (g) H<sub>2</sub>NOMe, pyridine, rt.

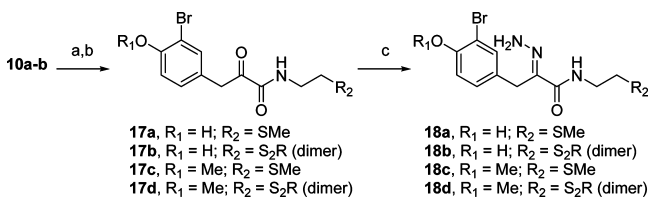
unit, and therefore the synthetic route will not be discussed in depth here.<sup>36</sup> Briefly, aromatic aldehydes 9a–n were converted in two steps to the corresponding arylpyruvic acids 10a–p. Condensation of 10a–p with *O*-(tetrahydro-2*H*-pyran-2-yl)-hydroxylamine<sup>37</sup> in pyridine, followed by EDCI-mediated coupling with the appropriate nucleophile and final THP-deprotection afforded oxime analogues 11a–d,i–x. Condensation of 10a,b (R<sub>1</sub> = 3-Br-4-OH and 3-Br-4-OMe, respectively) with *O*-methoxyamine in pyridine followed by EDCI-mediated coupling afforded *O*-methyloxime analogues 11e–h. It is noteworthy that only one final purification by flash column chromatography was necessary for the synthesis of *O*-methyloxime analogues, and two throughout the synthesis of oxime analogues. Compounds 11y and 11z were prepared according to an alternative procedure developed in our laboratory, as detailed previously.<sup>36</sup> Detailed structures are given in Tables 1 and 2. The oxime geometry of final compounds was assigned as (*E*) in each case, based on the NMR chemical shifts of the benzylic protons and the corresponding carbon atom.<sup>24,38–40</sup>

Table 2. Influence of Aromatic Substitution on Potency<sup>a</sup>

compd	R <sub>1</sub>	R <sub>2</sub> <sup>b</sup>	rHDAC1 IC <sub>50</sub> [μM]	rHDAC6 IC <sub>50</sub> [μM]	IC <sub>50</sub> <sup>6/1 c</sup>
11c'	3-Br-4-OH	SH	0.0009	0.36	400
11d'	3-Br-4-OMe	SH	0.0018	3.2	1778
11i'	—	SH	0.012	3.3	275
11j'	4-OH	SH	0.004	1.7	425
11k'	4-F	SH	0.007	2.9	414
11l'	4-SMe	SH	0.002	1.3	650
11 m'	3- <i>I</i> -4-OMe	SH	0.001	0.24	240
11n'	3-Br-4-F	SH	0.001	0.64	640
11o'	3-Br-4-SMe	SH	0.00048	0.19	396
11p'	3- <i>I</i> ,4,5-OMe	SH	0.001	0.27	270
11q'	3-Br-4,5-OMe	SH	0.001	0.51	510
11r'	3,4-OMe	SH	0.003	2.7	900
11s'	3-NO <sub>2</sub>	SH	0.001	1.2	1200
11t'	3-Br-5-NO <sub>2</sub>	SH	0.005	0.74	148
11u'	3,5-Br-4-OH	SH	0.0002	0.79	3950
11v'	3-OMe-4-SMe	SH	0.0006	1.4	2333
11y'	4-NMe <sub>2</sub>	SH	0.001	2.3	2300
11z'	3-Br-4-NMe <sub>2</sub>	SH	0.004	0.70	175

<sup>a</sup>IC<sub>50</sub> values for synthetic psammaplin A analogues (reduced form) against HDAC1 and HDAC6. <sup>b</sup>Thiols were prepared by in situ reduction of the respective disulfides using tris(2-carboxyethyl)phosphine hydrochloride and used immediately (see Experimental Section for details). Data for the corresponding disulfides are given in the Supporting Information. <sup>c</sup>IC<sub>50</sub><sup>6/1</sup> is defined by the ratio IC<sub>50</sub><sup>HDAC6</sup>/IC<sub>50</sub><sup>HDAC1</sup>.

The synthesis of  $\alpha$ -ketoamide-containing analogues **17a–d** was achieved using Py-BOP as the coupling reagent (Scheme 2). Whereas coupling of acids **10a** and **10b** with methyl-

Scheme 2. <sup>a</sup>

<sup>a</sup>Reagents and conditions: (a) **13** or **14** (free amine), DIPEA, THF, rt; (b) Py-BOP; (c) hydrazine monohydrate, MeOH, reflux.

thioethanamine **13** afforded analogues **17a** and **17c** in moderate yields, coupling with cystamine afforded dimeric compounds **17b** and **17d** in poor yields. Despite an intensive search for a more reliable route to these compounds, no significant yield improvement was made. Indeed, standard carbodiimide coupling conditions were found to be unsuccessful, leading to low and nonreproducible yields and purity. Other common coupling agents/conditions such as carbonyldiimidazole, isobutyl chloroformate, POCl<sub>3</sub>, oxalyl chloride, and thionyl chloride gave rise to degradation of the starting material. Further experimentation revealed the enolic form of the starting arylpyruvic acids to be acting as a competitive nucleophile, hampering the reaction. For example, treatment with DCC or isobutyl chloroformate mostly led to dehydration of the enol and protection as a carbonate, respectively. Carbonate deprotection was found capricious, therefore not representing a viable alternative to the use of Py-BOP.

$\alpha$ -Hydrazoneamide-containing analogues **18a–d** were prepared in moderate to good yields from ketoamides **17a–d** (Scheme 2). Heating **17a–d** in MeOH in the presence of hydrazine monohydrate afforded compounds **18a–d** as single isomers. The geometry of the hydrazone was determined as (*E*) in each case, based on NOE studies with analogue **18b** (see Supporting Information). Indeed, strong correlation between the hydrazone hydrogens and hydrogens H<sub>D</sub> was clearly observable (Figure 2, left), in addition to weak but visible

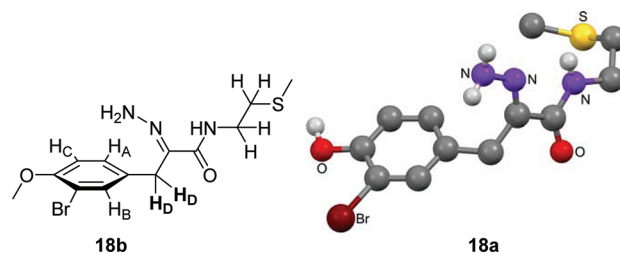
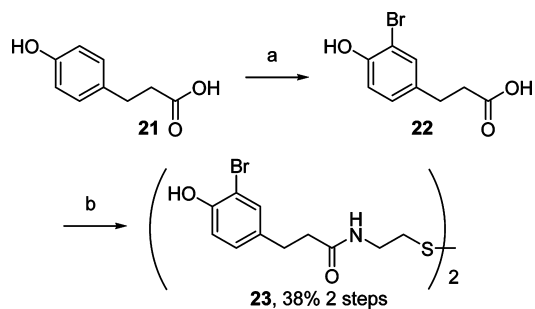


Figure 2. Determination of the geometry of the hydrazone unit in **18a–d**. NOE experiments with analogue **18b** (left), and X-ray crystal structure of analogue **18a** (right).

correlation with H<sub>A</sub> and H<sub>B</sub>. These results were finally confirmed by the X-ray crystal structure of compound **18a** (Figure 2, right).

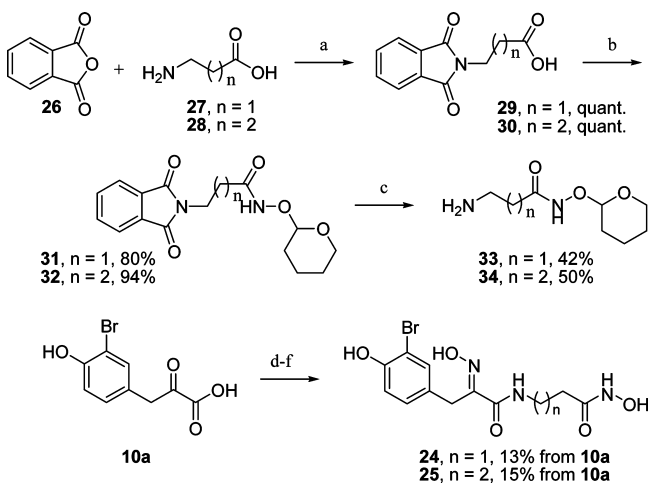
To study further the importance of the oxime unit of **11c** for potency against HDACs and DNMTs, an analogue of **11c** lacking the oxime unit was prepared (Scheme 3). Bromination of 3-(4-hydroxyphenyl)propanoic acid **21** afforded **22** as a 1:0.3 mixture of monobrominated compound **22** and its dibrominated analogue. Subsequent coupling with cystamine **14** using EDCI and HOBT as coupling reagents afforded simple analogue **23** in 38% yield over two steps. Reaction conditions for both

Scheme 3. <sup>a</sup>

<sup>a</sup>Reagents and conditions: (a)  $\text{Br}_2$ , AcOH, rt; (b) EDCI, HOBT,  $\text{CH}_2\text{Cl}_2$ , rt; (c) 14,  $\text{NEt}_3$ , rt.

bromination and coupling were not optimized, suggesting that improved yields should be achievable.

Because in terms of HDAC inhibition previous studies have postulated the sulfur end group of 11c (following prior reduction to the thiol) to function as a zinc binding group,<sup>34,35</sup> we decided to also prepare a hydroxamic acid hybrid analogue of psammaplin A 24 and its one-carbon homologue 25 (see Scheme 4). Hydroxamic acids are well-known to be suitable

Scheme 4. <sup>a</sup>

<sup>a</sup>Reagents and conditions: (a) 170–180 °C; (b) 12, EDCI, DMAP,  $\text{CHCl}_3$ , rt; (c) hydrazine hydrate, MeOH, reflux; (d) 12, pyridine, rt; (e) EDCI, NHS, dioxane, rt; (f) 33 or 34,  $\text{NEt}_3$ , dioxane/MeOH, rt; (g) 0.5 M HCl, 9:1 dioxane/iPrOH, rt.

zinc binding groups for HDACs,<sup>41</sup> and therefore we envisaged that 24 and 25 would provide useful information regarding the psammaplin A (HDAC) pharmacophore. Heating 3-aminopropanoic acid 27 or 4-aminobutanoic acid 28 in the presence of phthalic anhydride 26 in solvent-free conditions afforded protected intermediates 29 and 30 in nearly quantitative yield (Scheme 4).<sup>42</sup> Further EDCI-mediated coupling afforded intermediates 31 and 32 in high yield. Phthalimide deprotection then afforded primary amines 33 and 34 in moderate yield. Analogues 24 and 25 were then obtained in moderate yield after condensation of 10a with *O*-(tetrahydro-2H-pyran-2-yl)hydroxylamine 12, further amide coupling with 33 or 34, and final THP deprotection.

**Biological Assessment.** *HDAC Inhibition.* HDAC assays were performed as described by Wegener et al.<sup>43</sup> with minor

modifications. Our synthetic analogues were assayed against recombinant human HDAC1 (rHDAC1, class I), recombinant human HDAC6 (rHDAC6, class II), and purified bacterial histone deacetylase such as amidohydrolase (HDAH)<sup>44,45</sup> which exhibits 35% sequence identity with the second domain of the human HDAC6. The results are shown in Table 1.

As previously mentioned, 11c has been reported by Crews to be a potent inhibitor of HDAC activity (4.2 nM on a cell extract). Indeed, in our hands, 11c was found to be a potent HDAC1 inhibitor (11c, 45 nM), albeit less potent than previously reported, using a recombinant enzyme rather than cell extract.<sup>22</sup> Reference compound 4 displayed an  $\text{IC}_{50}$  of 30 nM, in close accord with previously reported values (27 nM).<sup>46</sup> Importantly, 11c was found to be 62-fold more potent against HDAC1 (45 nM) compared to the class II HDAC6 (2.8  $\mu\text{M}$ ). There is a pressing need for isoform-selective HDAC inhibitors to further validate these important targets, with most of the known inhibitors being non- or class-selective.<sup>4,47</sup> Previously, 11c was defined as a Class I-selective inhibitor by Kwon and co-workers, through its selective effects of histone acetylation (versus tubulin acetylation) in HeLa cells. To the best of our knowledge, our data provides the first class selectivity profile of 11c and analogues in cell-free assays. In Table 1,  $\text{IC}_{50}^{6/1}$  is defined by the ratio  $\text{IC}_{50}^{\text{HDAC6}}/\text{IC}_{50}^{\text{HDAC1}}$  and was used as an indicator of isoform selectivity.

The SAR around our library can be described as follows:

*Nature of the Sulfur End Group.* Because previous studies have postulated 11c to be a natural prodrug, whereby the disulfide functionality is reduced in cells to give a free thiol that functions as a zinc binding group,<sup>34,35</sup> we considered it important to assay the corresponding thiol directly. Indeed, direct cell-free assays of reduced psammaplin A analogues have not been previously reported. Thus all monomeric compounds ( $\text{R}_2 = \text{SH}$ ) were prepared immediately prior to assay from the corresponding disulfide analogues ( $\text{R}_2 = \text{SR}$  dimer), using tris(2-carboxyethyl)phosphine hydrochloride (TCEP) as the reducing agent, in a 9:1 DMSO/water solution (see Supporting Information). Importantly, control experiments have shown TCEP to have no influence in our assay conditions at concentrations up to 25  $\mu\text{M}$ . When the sulfur end group was present as a free thiol ( $\text{R}_2 = \text{SH}$ , 11c', 11d', 11g', 11h', 17c', 17d', 18c', 18d', 23'), highly potent compounds were observed in each case, efficiently inhibiting HDAC1 in the nanomolar range, while still showing important isoform selectivity. The impressive selectivity of these compounds was found to be particularly accentuated in the case of oxime (AB = NOH)- and hydrazone (AB = NNH<sub>2</sub>)-containing compounds 11c'/11d' and 18c'/18d', respectively, which were found to be highly selective for HDAC1 over HDAC6. The reduced natural product 11c' was found to be the most potent HDAC1 inhibitor of this series ( $\text{IC}_{50}$  of 0.9 nM), 50 fold more potent than its dimeric parent 11c (45 nM). Overall the disulfide analogues 11c,d,g,h, 17c,d, 18c,d, and 23 were found to be less potent than their reduced counterparts in every case. "Protection" of the free thiol as a thioether had a dramatic effect on potency. Analogues containing a thioether end group ( $\text{R}_2 = \text{SMe}$ , 11a, 11b, 11e, 11f, 17a, 17b, 18a, 18b) displayed low to no inhibition of both HDAC1 and HDAC6. Finally, hydroxamic analogue 24 was found to be highly potent against HDAC1 (2 nM) and HDAC6 (190 nM) with a similar potency to the thiol 11c' derived from 11c. Hydroxamic acid 25 was found to be less potent than 24, demonstrating the importance of the alkyl chain length for high potency.

**Requirement of the Oxime Functionality (AB).** Among the different AB systems tested (Table 1), the hydrazone compounds **18c'** (5 nM) and **18d'** (6 nM) were found to retain high potency against HDAC1, with values approaching those of their respective oxime analogues **11c'** (0.9 nM) and **11d'** (1.8 nM). Compounds **11g'** (27 nM) and **11h'** (15 nM), bearing an *O*-methyloxime moiety (AB = NOMe), were found to be 8–30 fold less active against HDAC1 compared to their respective oxime-containing analogues **11c'** (0.9 nM) and **11d'** (1.8 nM), suggesting the requirement of a free oxime for potent HDAC1 inhibition. Indeed, ketone analogues (AB = O) **17c'** (0.40  $\mu$ M) and **17d'** (1.1  $\mu$ M) were found to be 444 and 611 times less potent against HDAC1, respectively, than their corresponding oxime-containing analogues **11c'** (0.9 nM) and **11d'** (1.8 nM). Moreover, **17c'** and **17d'** were found to be in the same range of potency as **23'** (0.42  $\mu$ M), for which the AB functionality had been removed completely.

Interestingly, variation of the AB system had little effect on potency against HDAC6, despite its impact on potency against HDAC1. This possibly suggests a design criterion for isoform selectivity. Indeed, while analogue **23'** (AB = H<sub>2</sub>) and the  $\alpha$ -ketoamide-containing compounds (AB = O, **17c'** and **17d'**) did not significantly discriminate between HDAC1 and HDAC6, introduction of the *O*-methyloxime functionality induced a 15–73 increase in potency against HDAC1, while maintaining a similar potency against HDAC6. This effect is even more accentuated in the case of oxime-containing analogues **11c'** and **11d'** (AB = NOH) and hydrazone analogues **18c'** and **18d'** (AB = NNH<sub>2</sub>), which were 444–611 and 80–183 fold more potent, respectively, than **17c'**, **17d'**, and **23'** against HDAC1, while being similarly potent against HDAC6.

**Phenol Methylation Status.** Compounds bearing a methylated phenol (R<sub>1</sub> = Me, Table 1) led to similar potencies against HDAC1 compared to the corresponding free phenol (R<sub>1</sub> = H) in each case. Methylation of **11c'** and **11g'** led to compounds **11d'** and **11h'** which were 9 and 12 times less active, respectively, against HDAC6, whereas this pattern was found reversed for **17c'** and **18c'** which were found to be 4 and 3 times less potent, respectively, than their corresponding methylated analogues.

While this data is limited to HDAC1 and HDAC6, several representative compounds were also assayed against HDAH.<sup>44,45</sup> Surprisingly, all our synthetic analogues were found to be completely inactive under the assay conditions, even at concentrations of up to 100  $\mu$ M. The exceptions to this rule were the hydroxamic analogues **24** and **25**. For example, compound **25** was found to be significantly potent against HDAH (310 nM).

We then further explored the effects of aromatic substitution patterns on HDAC potency and selectivity. For clarity, only the results for the free thiol derivatives are given in Table 2, which were once again found to be more potent than their dimeric counterparts (see Supporting Information). The unsubstituted compound **11i'** was found to be the least active against both HDAC1 and HDAC6. Despite this, compound **11i'** (IC<sub>50</sub> of 12 nM) was still more potent than the reference compound **4** (30 nM, lit. 27 nM).<sup>50</sup> Importantly, several compounds exhibited subnanomolar IC<sub>50</sub> values against HDAC1: **11v'** (0.6 nM), **11o'** (0.48 nM) and the extremely potent compound **11u'** (0.2 nM). To the best of our knowledge, compound **11u'** represents the most potent HDAC1 inhibitor not involving a cyclic peptide motif. This compound also exhibited the highest selectivity with an IC<sub>50</sub><sup>6/1</sup> ratio of 3950. Analogue **11u'** was found to be 60

times more active than unsubstituted analogue **11i'** and demonstrates that aromatic substitution plays a role for potency against HDAC1. However, its influence on potency is minor compared to the presence of the free thiol or the free oxime.

Several important trends emerged from the HDAC6 assays. Compounds **11p'** (0.27  $\mu$ M), **11m'** (0.24  $\mu$ M), and **11o'** (0.19  $\mu$ M) were found to be more potent than the reduced form of **11c'** (0.36  $\mu$ M). The most potent compounds were found to involve a halogen in the meta position. This can be clearly seen by comparing the IC<sub>50</sub> values ( $\mu$ M) for **11k'** (2.9) vs **11n'** (0.64), **11r'** (2.7) vs **11q'** (0.51) and **11p'** (0.27), **11y'** (2.3) vs **11z'** (0.7), **11j'** (1.7) vs **11c'** (0.36), **11l'** (1.3) vs **11o'** (0.19) and **11s'** (1.2) vs **11t'** (0.74). In each case, the presence of a halogen was found to enhance potency against HDAC6. Moreover, iodinated compounds **11p'** (0.27) and **11m'** (0.24) were found to be more potent than their respective brominated analogues **11q'** (0.51) and **11d'** (3.2). Comparison of the IC<sub>50</sub> values ( $\mu$ M) for **11d'** (3.2), **11z'** (0.7), **11n'** (0.64), **11c'** (0.36), and **11o'** (0.19) enabled a preliminary ranking of functional groups in the para position to be made: OMe < NMe<sub>2</sub> < F < OH < SMe. Indeed, comparison of IC<sub>50</sub> values ( $\mu$ M) for the corresponding para-monosubstituted compounds **11k'** (2.9), **11y'** (2.3), **11j'** (1.7), and **11l'** (1.3) confirms this trend, indicating that the hydroxyl and thiomethylether substituents are most favorable in the para position for potency against HDAC6.

In light of the promising isoform selectivity of some of our library compounds, we decided to further investigate this effect for selected derivatives. The reduced form of psammaplin A **11c'**, its hydrazone-containing analogue **18c'**, and the hydroxamic analogue **24** were chosen as representative compounds. The compounds were assayed against rHDAC1 and rHDAC8 as Class I representatives, rHDAC6 as representative of class IIb, and rHDAC7 as representative of class IIa. The results are shown in Table 3. All compounds

**Table 3. HDAC Isoform Selectivity Profile of 11c', 18c', and 24**

compd <sup>a</sup>	AB	rHDAC1 IC <sub>50</sub> [ $\mu$ M]	rHDAC6 IC <sub>50</sub> [ $\mu$ M]	rHDAC7 IC <sub>50</sub> [ $\mu$ M]	rHDAC8 IC <sub>50</sub> [ $\mu$ M]
<b>11c'</b>	NOH	0.001	0.36	17	1.3
<b>18c'</b>	NNH <sub>2</sub>	0.005	1.0	45	13
<b>24</b>	NOH	0.002	0.19	33	1.5

<sup>a</sup>Thiols were prepared by in situ reduction of the respective disulfides using tris(2-carboxyethyl)phosphine hydrochloride and used immediately (see Experimental Section for details).

displayed similar selectivity profiles, with high selectivity for HDAC1. Indeed, the order of potency is HDAC1  $\gg$  HDAC6 > HDAC8 > HDAC7. Interestingly, all three compounds displayed isoform selectivity within the Class I HDACs (HDAC1 versus HDAC8). While having previously been shown to be less potent against the Class IIb HDAC6, all three compounds were also found to have only weak activity against the Class IIa HDAC7.

**Docking and Molecular Dynamics Simulations for HDAC Inhibition.** Because our data were consistent with the postulate that **11c** is a natural prodrug, with the free thiol functioning as a zinc binding group, we initiated computational studies to study its interactions with HDAC1. Recently, de Lera and co-workers performed preliminary computational studies

on the binding of **11c** to HDACs, using the crystal structure of HDAC8.<sup>35</sup> It would seem that in light of our isoform selectivity data (Table 3), HDAC8 is not a particularly suited model to study the binding of **11c**. Recently, the X-ray structure of HDAC2 in complex with a small-molecule ligand was solved<sup>48</sup> (PDB entry 3MAX), and because HDAC1 and HDAC2 are 93.7% identical for a 318 amino acid overlap, homology modeling of HDAC1 based on the 3D-structure of HDAC2 should provide a realistic structural model of HDAC1. Following construction of our HDAC1 homology model, computational docking studies were carried out on the psammaplin A monomer **11c'**, with the best pose selected for molecular dynamics calculations. After in vacuo minimization using steepest-descent and conjugate-gradient algorithms, the complex consisting of HDAC1 and **11c'** was solvated in a TIP4 water box and 250 mM NaCl. A position-restrained molecular dynamics simulation was run to equilibrate the water around the protein and to optimize the position of water molecules and ligand within the active site of the enzyme, followed by a 2 ns simulation at 300 K.

The modeling suggests that the psammaplin A monomer **11c'** forms three hydrogen bridges to Y303 (64%), D99 (77%), and the protonated H141 (26%) (Figure 3). The percentages

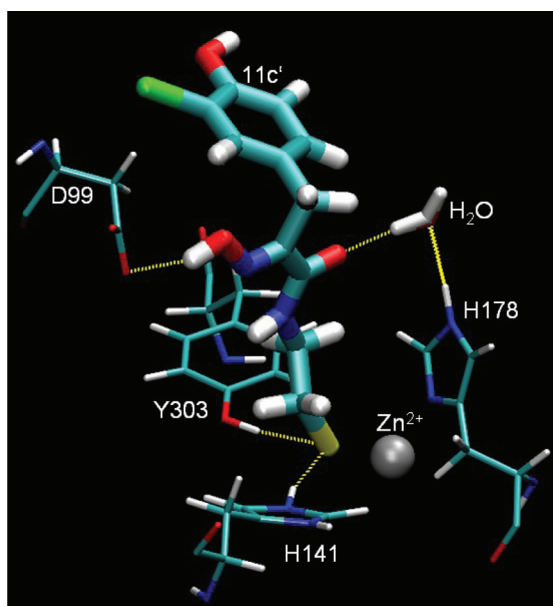


**Figure 3.** Snapshot of MD simulation of **11c'** in complex with HDAC1 (homology model). **11c'** forms hydrogen bonds (dotted yellow lines) with Y303, H141, and D99. A structural water molecule forms bridged hydrogen bonds with inhibitor and H178.

in brackets denote the fractional period of simulation where the hydrogen bonds are formed. In addition, a structural water molecule with extraordinary restrained position appeared during the simulation. This water molecule bridges the amide-oxygen of **11c'** and H178. The hydrogen bond between the ligand and this water molecule is formed through 96% of the simulation run whereas the hydrogen bond between the ligand and H178 is stable for about 50% of the run period. Moreover, a strong interaction between the thiolate and the catalytic  $Zn^{2+}$  ion is predicted, with a very sharp radial pair distribution between  $Zn^{2+}$  and the sulfur atom of the ligand with a mean distance of  $(2.0 \pm 0.1) \text{ \AA}$ .

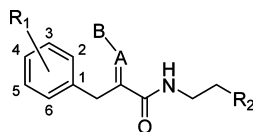
**DNMT1 Inhibition.** Because there are few reports of small molecule, non-nucleoside DNMT inhibitors in the literature, we were particularly interested to assess the DNMT activity of our libraries. Despite the initial report by Crews and co-workers that **11c** is highly potent against semipurified DNMT1 ( $18.6 \text{ nM}$ ),<sup>22</sup> recent studies by de Lera and co-workers observed no inhibition of DNMT1 immunoprecipitated from K562 cells or recombinant DNMT3a.<sup>35</sup> We therefore considered that we could further study the potential for DNMT1 inhibition using our high-throughput fluorescence intensity assay (see Experimental Section for details).

Disappointingly, none of our synthetic analogues assessed showed significant inhibition of DNMT1 at  $30 \text{ }\mu\text{M}$  (see Supporting Information). The dimeric analogues were also assayed as free thiols, but no significant inhibition could be observed, even at  $120 \text{ }\mu\text{M}$ . One potential concern was the reductive assay conditions required ( $5 \text{ mM DTT}$ ), which would result in the reduction of any disulfide analogues assessed. Should it be the parent dimeric structure that was active, it is likely this would not be present under the assay conditions. Analogues **11w**<sup>35</sup> and **11x** (obtained from diamines **15** and **16**, respectively, Scheme 1) were prepared (vide supra) to replace the native disulfide functionality of **11c** with two methylene groups and a thioether, respectively (Scheme 1). Such analogues should be chemically stable under the assay conditions. Unfortunately, **11w** and **11x** were also found inactive against DNMT1. *S*-Adenosyl homocysteine (SAH) was used as a positive control in the assay, which gave an  $IC_{50}$  of  $0.9 \text{ }\mu\text{M}$  ( $160$  replicates, lit.  $2\text{--}4 \text{ }\mu\text{M}$ ,<sup>49,50</sup> (see Supporting Information)).

As an alternative assay, we decided to study the effects of **11c** and its reduced form (**11c'**) on the M.SssI bacterial methyltransferase. This is a widely used model to study the effects of DNA methylation on mammalian genomes, because this bacterial enzyme is structurally related to mammalian DNA methyltransferases and recognizes the same sequence (CpG).<sup>51</sup> Indeed, it has been previously used as the basis of an in vitro model to study the activities of inhibitors of mammalian methyltransferases.<sup>52,20</sup> Furthermore, Sufrin and co-workers have previously reported **11c** to inhibit bacterial methyltransferases.<sup>53,19</sup> Both **11c** and its reduced form **11c'** were found to potently inhibit M.SssI methyltransferase at  $50 \text{ }\mu\text{M}$  (see Supporting Information). The assay was repeated four times, including positive and negative controls, and in each case **11c** and the reduced form **11c'** were seen to inhibit M.SssI methyltransferase activity equivalently down to  $5 \text{ }\mu\text{M}$ .

**Cell-Based Studies of Psammaplin A Analogues.** A large selection of compounds from our library were assessed for cytotoxicity against A549 (human lung carcinoma), MCF7 (human breast carcinoma), and WI38 (normal human lung fibroblast) cell lines. Representative results are given in Table 4. Methylthioether-containing analogues **11a**, **11e**, **17a**, and **18a** were found almost inactive against the three cell lines tested. The majority of the disulfides and thiols exhibited micromolar activities. Compound **11d'** was found particularly active ( $0.16 \text{ }\mu\text{M}$  against A549,  $0.61 \text{ }\mu\text{M}$  against MCF7). Interestingly, thiol **18c'** was found particularly selective against MCF7 ( $3.42 \text{ }\mu\text{M}$ ) with a 10-fold increase in potency compared to the other cell lines. Hydroxamic acid **24** displayed significant cytotoxicity toward all three cell lines.

To investigate the isoform selectivity of **11c** and analogue **24** in cells, Western blot analysis was performed in MCF7 cells, with trichostatin A (TSA, **1**) used as a positive control.<sup>54</sup>

Table 4. Cytotoxicity Data of Psammaplin A Analogues<sup>a</sup>

compd	R <sub>1</sub>	AB	R <sub>2</sub> <sup>b</sup>	A549 GI <sub>50</sub> [μM]	MCF7 GI <sub>50</sub> [μM]	WI38 GI <sub>50</sub> [μM]
11a	3-Br-4-OH	NOH	SMe	>50	>50	>50
11c	3-Br-4-OH	NOH	S <sub>2</sub> R (dimer)	7.5	1.27	3.44
11c'	3-Br-4-OH	NOH	SH	2.53	2.35	3.4
11d'	3-Br-4-OMe	NOH	SH	0.16	0.61	1.13
11e	3-Br-4-OH	NOMe	SMe	>50	>50	>50
11g	3-Br-4-OH	NOMe	S <sub>2</sub> R (dimer)	49.5	nd	>50
11g'	3-Br-4-OH	NOMe	SH	10.6	19.3	24.2
17a	3-Br-4-OH	O	SMe	>50	18.3	nd
17c	3-Br-4-OH	O	S <sub>2</sub> R (dimer)	15.2	13.1	33.1
17c'	3-Br-4-OH	O	SH	43	35.4	42.6
18a	3-Br-4-OH	NNH <sub>2</sub>	SMe	>50	>50	>50
18c	3-Br-4-OH	NNH <sub>2</sub>	S <sub>2</sub> R (dimer)	18.8	3.81	nd
18c'	3-Br-4-OH	NNH <sub>2</sub>	SH	33.4	3.42	37.2
11i	–	NOH	S <sub>2</sub> R (dimer)	16.3	11.1	>50
11i'	–	NOH	SH	15.2	9.38	10.9
11n	3-Br-4-F	NOH	S <sub>2</sub> R (dimer)	2.73	1	1.8
11n'	3-Br-4-F	NOH	SH	6.24	2.87	7.72
11q	3-Br-4,5-OMe	NOH	S <sub>2</sub> R (dimer)	2.51	0.72	2.14
11q'	3-Br-4,5-OMe	NOH	SH	4.4	2.25	4.31
24	3-Br-4-OH	NOH	C(O)NHOH	1.59	1.13	7.86
TCEP				>50	>50	>50

<sup>a</sup>Psammaplin A and synthetic analogues (selected examples) display micromolar cytotoxicity against A549, MCF7, and WI38 cell lines. <sup>b</sup>Thiols were prepared by in situ reduction of the respective disulfides using tris(2-carboxyethyl)phosphine hydrochloride and used immediately (see Experimental Section for details). Additional cytotoxicity data are available in Supporting Information.

Untreated cells were used as a negative control. Variations in the protein levels of acetylated histone H3 (Ac-H3), histone H3 (H3), acetylated tubulin (Ac-tubulin), tubulin, and p21 were studied. The results are shown in Figure 4. Compounds

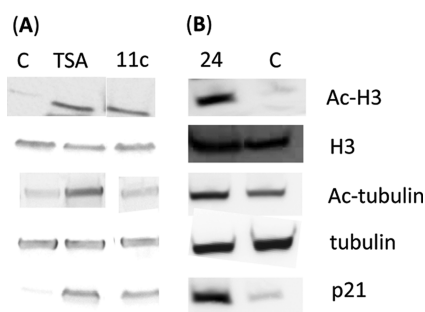


Figure 4. Western blot analyses of MCF7 cells after 24 h of treatment with: TSA (0.5 μM); 11c' (5 μM), and 24 (1 μM).

11c, 24, and TSA were all found to induce up-regulation of Ac-H3, in accordance with their inhibitory potency toward HDAC1. Furthermore p21 up-regulation, which is known to be a downstream effect of Class I HDAC inhibition,<sup>55</sup> was also observed. Importantly, while TSA had a strong effect on tubulin acetylation, a known target of HDAC6, no significant effect was observed for 11c. Similarly, at a concentration of 1 μM, hydroxamic analogue 24 had only a minimal effect on tubulin acetylation. This data is in agreement with the isoform selectivity data observed in cell-free assays.

## DISCUSSION

**HDAC Inhibitory Activity and Selectivity of 11c and Analogues.** It has been previously reported by Kwon and co-workers that in terms of its HDAC activity, 11c functions as a natural prodrug, the active free thiol being revealed following disulfide reduction in vivo.<sup>34</sup> The evidence for this proposal is that pretreatment of both 11c and HDAC1 with H<sub>2</sub>O<sub>2</sub> as an oxidant leads to low level inhibition of HDAC activity,<sup>34</sup> coupled with the decreased potency of 11c against glutathione-deficient cells. Recently, an analogous proposal was presented by de Lera and co-workers based on the fact that a psammaplin A analogue lacking the disulfide bond (11w) was inactive, as were analogues where the disulfide unit was replaced by methyl ether, methyl thioether and alcohol functionalities.<sup>35</sup> Similar conclusions have been drawn for other disulfide bearing cyclic peptidic natural products, such as the HDAC inhibitor FK228.<sup>56</sup> Because the common pharmacophore of most HDAC inhibitors contains a zinc-binding end group (ZBG), and the fact that thiols are known to be excellent ligands for zinc,<sup>41</sup> we felt the prospect of a free thiol as the active species to be highly plausible. Indeed, synthetic HDAC inhibitors utilizing thiol zinc binding groups (protected as thioesters) have been previously reported.<sup>57</sup>

The SAR described for our psammaplin A-derived libraries is in accord with the hypothesis that 11c is first reduced to the monomeric thiol, and this corresponding monomer is the active HDAC inhibitor. Indeed, by directly assaying the free thiol species, we unambiguously observed the potent inhibitory activity of these compounds. In contrast, the corresponding methyl thioethers were not active at all. A parallel observation



was previously made by Horinouchi and co-workers during their study of FK228.<sup>56</sup> Furthermore, our attempts at computational docking studies with the dimeric disulfide structure of **11c** and the active site of HDAC enzymes such as HDLP (1C3P, 1C3R, 1C3S), HDAC2 (3MAX), HDAC8 (1T64, 3F0R, 1T69), HDAC4 (2VQJ, 2VQM), HDAC7 (3C10, 3C0Z), or HDAH (1ZZ1, 1ZZ3, 1ZZ0, 2VCG) revealed no suitable binding poses. As described above, a compatible binding model which fits our SAR was instead obtained for the monomeric thiol (vide supra, Figure 3). What is unclear, however, is why the parent disulfide analogues retain any potency in *cell-free* assays. While this may be related to their ability to generate thiols in situ (via reduction or thiol exchange) under the assay conditions, the precise mechanism is still unclear. Indeed, to check whether contamination of the dimeric disulfides with their thiol counterparts was producing the inhibitory effects, we incubated **11c** and **11d** in the presence of hydrogen peroxide prior to the assay (5 mM disulfide, 1% H<sub>2</sub>O<sub>2</sub>, 90 min in the dark, and then dilution to 5 μM and further dilutions for assay). The resultant IC<sub>50</sub> values for **11c** and **11d** showed a loss in potency. The enzyme activity was found unaffected by the presence of H<sub>2</sub>O<sub>2</sub>. This result confirms the preliminary results obtained by Kwon and co-workers<sup>34</sup> and strongly suggests the thiol as the active species.

As final confirmation of the monomeric thiol species being the active compound, we found hydroxamic acid analogue **24** to be a highly potent HDAC1 inhibitor. Not only does this illustrate the compatibility of the hydroxamic acid group with the hydroxiimino bromotyrosine-based scaffold of **11c**, but it also supports the hypothesis that the thiol end group is functioning as a zinc-binding group for HDAC inhibition. The one caveat is that in contrast with hydroxamic acids **24** and **25**, all thiols tested were found very weakly active against HDAH (IC<sub>50</sub> of **24**: 0.31 μM; IC<sub>50</sub> of **25**: 5.25 μM). Indeed, in our assay, **11c'** and **18c'** displayed IC<sub>50</sub>s of 30.2 μM and 32.0 μM, respectively, against HDAH. The reason for the lack of activity of thiols against HDAH is still unclear and is under further investigation.

One striking aspect of our data is the high selectivity of **11c** and many of our analogues for HDAC1. As described, the oxime functionality in **11c** appears to play an important role, not only in potency against HDAC1 but also in HDAC1 selectivity. Indeed, while ketone analogues **17c'** and **17d'** and compound **23'** bearing no functionality in this position displayed similar potencies against both HDAC1 and HDAC6, introduction of the oxime (and to a lower extent, the hydrazone) resulted in an increase in potency against HDAC1, while keeping potency against HDAC6 relatively unaffected. These results thus suggest a possible design criterion for HDAC1-selective inhibitors. At the molecular level, it is likely that the selectivity is due to structural differences between the active sites of class I and class II HDACs. While our binding model (Figure 3) is suggestive of an interaction between the oxime functionality and D99, D99 (HDAC1) is conserved through all members of zinc dependent HDACs, and therefore this interaction is not sufficient to explain isoform selectivity. We hypothesize that among other structural features, hydrogen bonding to Y303 contributes to selectivity because it is substituted by histidine in class II HDACs. This tyrosine is assumed to stabilize the oxyanion during the catalytic deacetylation process.<sup>58,59</sup> Indeed, crystal structures of enzyme–inhibitor complexes involving HDAC2 (3MAX), HDAC8 (1T64), and HDAH (1ZZ1) show hydrogen bonds between the hydroxyl group of the catalytic tyrosine and

the corresponding inhibitors. In contrast, in the crystal structures of enzyme–inhibitor complexes of HDAC4 (e.g., 2VQJ, 2VQM) and HDAC7 (3COZ, 3C10) the histidine residues corresponding to the catalytic tyrosine are rotated outward from the active site. Finally, L271 (HDAC1) is conserved through class II and class I HDACs apart from HDAC8, where leucine is replaced by methionine. This difference might contribute to the observed differences in substrate and inhibitor selectivities within class I between HDAC-1, -2, -3, and -8, as is seen for **11c** and analogues.

In terms of the substitution pattern of the aromatic “capping” unit, we found this feature to have less of an effect on potency and selectivity than the thiol or the oxime functionality. This is agreement with the SAR observed by de Lera and co-workers.<sup>35</sup> Our model (Figure 3) suggests that the aromatic ring is positioned at the entrance of the channel leading to the active site, potentially interacting with one or both of the conserved phenylalanines at the channel entrance.

**Methyltransferase Inhibitory Activity of 11c and Analogues.** **11c** and other members of the psammaphin family have been previously reported to be potent inhibitors of the human DNMT1 in vitro (IC<sub>50</sub> = 18.6 nM for **11c** against semipurified DNMT1).<sup>22</sup> In our DNMT1 assay, **11c** and all synthetic analogues were found inactive at concentrations of up to 30 μM and 120 μM (free thiols). This data is in agreement with the recent data reported by de Lera and co-workers, who reported the lack of potency of several psammaphin A analogues against immunoprecipitated DNMT1 in an alternative methyltransferase assay.<sup>35</sup> The origin of the disconnect between our data and the values reported by Crews and co-workers<sup>22</sup> is still unclear, but several differences in protein purity and the assay conditions are apparent. Crews and co-workers used semi-purified DNMT1, whereas highly purified enzyme was used in our assay. The methylation substrate (and its concentration) was also different in each case, with biotinylated poly(dI-dC) used by Crews and a hairpin DNA mimic oligo being used in our assay. It is germane to mention, however, that the de Lera study also used a poly(dI-dC) substrate and failed to observe activity.<sup>35</sup> Because most DNMT assays involve substantial quantities of reducing agents, usually DTT, to avoid degradation of the DNA substrate by external oxidative agents (such as O<sub>2</sub>) it is important to recognize chemical instability of our compounds (to reduction) under these conditions. Our results on the nonreducible analogues **11w**<sup>35</sup> and **11x** (vide supra), which were also found to be inactive, suggest, however, that chemical reduction of psammaphin A analogues is not responsible for the lack of potency against DNMT1. Taken together, the lack of activity observed in our in vitro assays, coupled with the lack of activity observed by de Lera and co-workers, lead us to question the activity of **11c** (and analogues) against DNMT1. While such a supposition is based on data from cell-free assays, it is important to highlight that Sufrin and co-workers, have reported a lack of DNA hypomethylation as a result of exposure of HCT116 human colon carcinoma cells to **11c**. **11c** also failed to induce the hypomethylation or reactivation of methylation-silenced genes.<sup>53,60</sup> Because **11c** has been reported to have low physiological stability,<sup>30,31,61</sup> it is plausible that the lack of an effect on DNA methylation in cells is due to transport and stability issues. An alternative explanation is that **11c** is largely inactive against human DNMTases.

Interestingly, **11c** was, however, found to inhibit the M.SssI bacterial methyltransferase at low micromolar concentrations

(see Supporting Information). This result is in accordance with preliminary data reported by Sufirin, who also reported activity against bacterial methyltransferases.<sup>53</sup> Importantly, while we observed that both **11c** and its reduced form were active against the bacterial methyltransferase, DTT contained in the buffer likely generated substantial amounts of reduced **11c** in situ regardless of how the compound was dosed. The mechanism of inhibition of bacterial methyltransferases is unclear at this point.

**Cellular Studies on Psammalin A.** Our synthetic analogues showed significant inhibition of cell growth against A549 (human lung carcinoma), MCF7 (human breast carcinoma), and WI38 (normal human lung fibroblast) cell lines (see Table 4). For example, several compounds were found to inhibit cell growth at submicromolar concentrations, including **11d'** (A549: 0.16  $\mu$ M, MCF7: 0.61  $\mu$ M) and **11q** (MCF7: 0.72  $\mu$ M). This data is in agreement with previous studies that have reported **11c** to have significant potency (ED<sub>50</sub>,  $\mu$ g/mL) against human lung (A549, 0.57), ovarian (SK-OV-3, 0.14), skin (SK-MEL-2, 0.13), CNS (XF498, 0.57), and colon (HCT15, 0.68) cancer cell lines.<sup>33</sup> Furthermore, it has been reported to cause G1 arrest in human endometrial Ishikawa cancer cells<sup>62</sup> and U937 leukemia cells,<sup>35</sup> which correlates with the effect of known HDAC inhibitors. We found that methylthioether-containing analogues **11a**, **11e**, **17a**, and **18a** (Table 4) were largely inactive against all cell lines tested, correlating with our SAR against HDAC inhibition. Additionally, compounds bearing an oxime motive (AB = NOH, Table 4) were found more potent than their respective analogues bearing an *O*-methyloxime (AB = NOME, Table 4) or ketone (AB = O, Table 4), once again correlating with SAR data previously obtained in HDAC assays. Taken together, this demonstrates that **11c** cytotoxicity correlates with HDAC inhibition.

HDAC1 knockdown in MCF-7 cells has been previously reported to result in cell cycle arrest in G1 and G2.<sup>63</sup> In light of the fact that our studies indicated **11c** to have significant potency and selectivity against HDAC1, and that HDAC inhibitors are being clinically evaluated for breast cancer treatment,<sup>64</sup> we decided to investigate further the mode of action of our inhibitors in MCF7 cells. Western blot analysis revealed **11c** and **24** to induce up-regulation of Ac-H3, correlating well with their HDAC inhibitory potency (Figure 4). The inability of **11c** to significantly up-regulate Ac-tubulin, a substrate for HDAC6, also correlates with the low inhibitory potencies of this compound against HDAC6 in vitro and therefore isoform selectivity. Furthermore, correlating to their Class I inhibitory potency, the cyclin-dependent kinase inhibitor p21 was also up-regulated. These results also correlate with those obtained by the de Lera group in U937 cells.<sup>35</sup> While the hydroxamic acid analogue **24** also had a much more dramatic effect on Ac-H3 than Ac-tubulin, the selectivity was less than that of **11c**, which correlates with the observed differences in selectivity in cell-free assays (Table 3). It has been previously highlighted that **11c** has low stability and that there are transport issues in vivo and in cells.<sup>35</sup> Indeed, we found the response by MCF7 cells to be highly dependent on the concentration of inhibitor used and the incubation time. No significant response was observed below an inhibitor (**11c**) concentration of 5  $\mu$ M, despite the high potency for HDAC1 inhibition observed in cell-free assays. Pleasingly, however, the hydroxamic analogue **24** gave a robust response down to 1  $\mu$ M (the lowest concentration tested). Although further exploration is required, it seems apparent that replacing the thiol zinc

binding group with a hydroxamic acid increases the compound stability in cells while broadly maintaining the isoform selectivity observed for the psammalin A scaffold.

## CONCLUSIONS

**11c** is a marine metabolite that was reported to have potent inhibitory activity against two independent epigenetic pathways, histone deacetylation and DNA methylation. Through systematic synthesis of a range of psammalin A analogues and subsequent biological assessment, we have probed the molecular functionality responsible for these reported effects. We have found **11c** to function as a potent HDAC inhibitor once reduced to its mimeric thiol precursor. While other studies have also highlighted this possibility,<sup>34,35</sup> we have for the first time directly assayed the corresponding thiols of psammalin A and analogues and found them to have low to subnanomolar inhibitory potency against HDAC1. Furthermore, using a small HDAC panel, we have observed a striking isoform selectivity profile for this natural product, being 360-fold selective for HDAC1 over HDAC6 and more than 1000-fold less potent against HDAC7 and HDAC8. Pleasingly, such selectivity seems retained in MCF7 cells, with histone acetylation significantly affected by compound treatment but tubulin acetylation (an HDAC6 substrate) unaffected. The SAR around our psammalin A library has highlighted the unusual oxime functionality to be important in this selectivity profile and indeed could suggest a design criterion for HDAC1-selective compounds. While it would seem that **11c** could therefore function as a useful chemical probe of HDAC1 in cells, its low cellular stability remains problematic. We have demonstrated, however, that the thiol zinc binding group can be replaced by other metal chelating units, such as a hydroxamic acid moiety, and the activity and isoform selectivity is broadly maintained. This result highlights compound **24** as a useful chemical probe molecule in biological studies targeting HDAC1. Finally, in agreement with others, we have found no evidence of DNMT1 activity for **11c** and therefore suggest this does not represent a viable start point for non-nucleoside DNMT inhibitors.

## EXPERIMENTAL SECTION

**Chemistry.** Compounds **10a–p** and **11a–z** were prepared according general procedures we have reported in a previous manuscript.<sup>36</sup> We recently reported on the synthesis and characterization of compounds **10a**, **10b**, **11c**, **11f**, **11s**, **11v**, **11y**, **11z**, 2-bromo-4-((2-methyl-5-oxoxazol-4(5H)-ylidene)methyl)phenyl acetate, 4-(3-bromo-4-methoxybenzylidene)-2-methyl-4H-oxazol-5-one, 2-methyl-4-(3-nitrobenzylidene)oxazol-5(4H)-one, and 4-(3-methoxy-4-(methylthio)benzylidene)-2-methyloxazol-5(4H)-one.<sup>36</sup> Acids **10c** and **10d** were obtained from Sigma Aldrich and were used without further purification. All compounds for biological assessment were >95% pure as determined by combustion analysis.

**4-(4-Fluorobenzylidene)-2-methyloxazol-5(4H)-one.** The title oxazolone (2.30 g, 54%) was prepared from 4-fluorobenzaldehyde **9c** and obtained as a yellow solid. <sup>1</sup>H NMR (400 MHz, CDCl<sub>3</sub>)  $\delta$  2.41 (s, 3H), 7.08–7.17 (m, 3H), 8.07–8.14 (m, 2H); <sup>13</sup>C NMR (100 MHz, CDCl<sub>3</sub>)  $\delta$  15.7, 116.1 (d,  $J_{CF}$  = 22.3 Hz), 129.5 (d,  $J_{CF}$  = 2.4 Hz), 130.0, 132.2, 134.3 (d,  $J_{CF}$  = 8.7 Hz), 164.2 (d,  $J_{CF}$  = 254.5 Hz), 166.2, 167.7; HRMS (ESI+)  $m/z$  calcd for C<sub>11</sub>H<sub>9</sub>FNO<sub>2</sub> [M + H]<sup>+</sup> 206.0612, found: 206.0612.

**2-Methyl-4-(4-(methylthio)benzylidene)oxazol-5(4H)-one.** The title oxazolone (3.20 g, 66%) was prepared from 4-methylthiobenzaldehyde **9d** and obtained as a light orange solid. <sup>1</sup>H NMR (400 MHz, CDCl<sub>3</sub>)  $\delta$  2.39 (s, 3H), 2.52 (s, 3H), 7.09 (s, 1H), 7.24–7.28 (m, 2H), 7.96–8.02 (m, 2H); <sup>13</sup>C NMR (100 MHz,

$\text{CDCl}_3$ )  $\delta$  14.8, 15.6, 125.5, 129.6, 131.0, 131.6, 132.4, 143.7, 165.4, 167.9; HRMS (ESI+)  $m/z$  calcd for  $\text{C}_{12}\text{H}_{12}\text{NO}_2\text{S}$  [ $\text{M} + \text{H}$ ] $^+$  234.0583, found: 234.0587.

**4-(3-Iodo-4-methoxybenzylidene)-2-methyloxazol-5(4H)-one.** The title oxazolone (3.70 g, 69%) was prepared from 3-iodo-4-methoxybenzaldehyde **9e** and obtained as an orange solid.  $^1\text{H}$  NMR (400 MHz,  $\text{CDCl}_3$ )  $\delta$  2.41 (s, 3H), 3.95 (s, 3H), 6.87 (d,  $J = 8.6$  Hz, 1H), 7.00 (s, 1H), 8.04 (dd,  $J = 8.6, 2.1$  Hz, 1H), 8.59 (d,  $J = 2.1$  Hz, 1H);  $^{13}\text{C}$  NMR (100 MHz,  $\text{CDCl}_3$ )  $\delta$  15.6, 56.5, 86.4, 110.6, 128.0, 129.4, 131.3, 134.1, 143.1, 160.1, 165.6, 167.7; HRMS (ESI+)  $m/z$  calcd for  $\text{C}_{12}\text{H}_{11}\text{INO}_3$  [ $\text{M} + \text{H}$ ] $^+$  343.9778, found: 343.9791.

**4-(3-Bromo-4-fluorobenzylidene)-2-methyloxazol-5(4H)-one.** The title oxazolone (4.00 g, 66%) was prepared from 3-bromo-4-fluorobenzaldehyde **9f** and obtained as a yellow solid.  $^1\text{H}$  NMR (400 MHz,  $\text{CDCl}_3$ )  $\delta$  2.42 (s, 3H), 7.01 (s, 1H), 7.18 (app-t,  $J = 8.4$  Hz, 1H), 7.98 (m, 1H), 8.39 (app-d,  $J = 5.5$  Hz, 1H);  $^{13}\text{C}$  NMR (100 MHz,  $\text{CDCl}_3$ )  $\delta$  15.7, 109.8 (d,  $J_{\text{CF}} = 22.3$  Hz), 116.9 (d,  $J_{\text{CF}} = 22.7$  Hz), 128.2, 130.9 (d,  $J_{\text{CF}} = 3.4$  Hz), 133.0 (d,  $J_{\text{CF}} = 7.6$  Hz), 133.2 (d,  $J_{\text{CF}} = 2.4$  Hz), 137.0, 160.3 (d,  $J_{\text{CF}} = 255.0$  Hz), 167.0, 167.3; HRMS (ESI+)  $m/z$  calcd for  $\text{C}_{11}\text{H}_8\text{BrFNO}_2$  [ $\text{M} + \text{H}$ ] $^+$  283.9717, found: 283.9727.

**4-(3-Bromo-4-(methylthio)benzylidene)-2-methyloxazol-5(4H)-one.** The title oxazolone (brown solid, 2.47 g, 37%) was prepared from 3-bromo-4-(methylthio)benzaldehyde **9g** and obtained as a yellow solid.  $^1\text{H}$  NMR (400 MHz,  $\text{CDCl}_3$ )  $\delta$  2.41 (s, 3H), 2.52 (s, 3H), 7.01 (s, 1H), 7.14 (d,  $J = 8.4$  Hz, 1H), 7.95 (dd,  $J = 8.4, 1.8$  Hz, 1H), 8.33 (d,  $J = 1.8$  Hz, 1H);  $^{13}\text{C}$  NMR (100 MHz,  $\text{CDCl}_3$ )  $\delta$  15.5, 15.7, 121.3, 124.4, 129.2, 130.5, 131.2, 132.5, 135.2, 144.3, 166.1, 167.5; HRMS (ESI+)  $m/z$  calcd for  $\text{C}_{12}\text{H}_{11}\text{BrNO}_2\text{S}$  [ $\text{M} + \text{H}$ ] $^+$  311.9688, found: 311.9689.

**4-(3-Iodo-4,5-dimethoxybenzylidene)-2-methyloxazol-5(4H)-one.** The title oxazolone (2.70 g, 90%) was prepared from 3-iodo-4,5-dimethoxybenzaldehyde **9h** and obtained as an orange solid.  $^1\text{H}$  NMR (400 MHz,  $\text{CDCl}_3$ )  $\delta$  2.41 (s, 3H), 3.90 (s, 3H), 3.92 (s, 3H), 6.97 (s, 1H), 7.84 (d,  $J = 1.8$  Hz, 1H), 7.96 (d,  $J = 1.8$  Hz, 1H);  $^{13}\text{C}$  NMR (100 MHz,  $\text{CDCl}_3$ )  $\delta$  15.7, 56.0, 60.6, 92.3, 115.7, 129.3, 131.1, 132.4, 135.2, 151.3, 152.4, 166.2, 167.5; HRMS (ESI+)  $m/z$  calcd for  $\text{C}_{13}\text{H}_{13}\text{INO}_4$  [ $\text{M} + \text{H}$ ] $^+$  373.9884, found: 373.9886.

**4-(3-Bromo-4,5-dimethoxybenzylidene)-2-methyloxazol-5(4H)-one.** The title Oxazolone (3.20 g, 70%) was prepared from 3-bromo-4,5-dimethoxybenzaldehyde **9i** and obtained as an orange solid.  $^1\text{H}$  NMR (400 MHz,  $\text{CDCl}_3$ )  $\delta$  2.41 (s, 3H), 3.92 (s, 3H), 3.93 (s, 3H), 6.98 (s, 1H), 7.77 (d,  $J = 1.8$  Hz, 1H), 7.80 (d,  $J = 1.8$  Hz, 1H);  $^{13}\text{C}$  NMR (100 MHz,  $\text{CDCl}_3$ )  $\delta$  15.7, 56.1, 60.8, 114.7, 117.7, 129.3, 129.4, 130.1, 132.6, 148.8, 153.5, 166.3, 167.5; HRMS (ESI+)  $m/z$  calcd for  $\text{C}_{13}\text{H}_{13}\text{BrNO}_4$  [ $\text{M} + \text{H}$ ] $^+$  326.0022, found: 326.0019.

**4-(3,4-Dimethoxybenzylidene)-2-methyloxazol-5(4H)-one.** The title oxazolone (3.60 g, 69%) was prepared from 3,4-dimethoxybenzaldehyde **9j** and obtained as a brown solid.  $^1\text{H}$  NMR (400 MHz,  $\text{CDCl}_3$ )  $\delta$  2.38 (s, 3H), 3.94 (s, 3H), 3.95 (s, 3H), 6.90 (d,  $J = 8.4$  Hz, 1H), 7.08 (s, 1H), 7.50 (dd,  $J = 8.4, 1.9$  Hz, 1H), 7.93 (d,  $J = 1.9$  Hz, 1H);  $^{13}\text{C}$  NMR (100 MHz,  $\text{CDCl}_3$ )  $\delta$  15.6, 55.9 (2C), 110.8, 113.8, 126.4, 127.3, 130.5, 131.6, 149.1, 151.9, 164.9, 168.1; HRMS (ESI+)  $m/z$  calcd for  $\text{C}_{13}\text{H}_{14}\text{NO}_4$  [ $\text{M} + \text{H}$ ] $^+$  248.0917, found: 248.0916.

**4-(3-Bromo-5-nitrobenzylidene)-2-methyloxazol-5(4H)-one.** The title oxazolone (1.91 g, 60%) was prepared from 3-bromo-5-nitrobenzaldehyde **9l** and obtained as a brown solid.  $^1\text{H}$  NMR (400 MHz,  $\text{CDCl}_3$ )  $\delta$  2.48 (s, 3H), 7.05 (s, 1H), 8.39 (app-t,  $J = 1.9$  Hz, 1H), 8.53 (app-t,  $J = 1.5$  Hz, 1H), 8.89 (app-t,  $J = 1.6$  Hz, 1H);  $^{13}\text{C}$  NMR (100 MHz,  $\text{CDCl}_3$ )  $\delta$  15.9, 123.2, 124.9, 125.8, 127.8, 135.9, 136.1, 139.7, 149.0, 166.5, 168.9; HRMS (EI+)  $m/z$  calcd for  $\text{C}_{11}\text{H}_7\text{BrN}_2\text{O}_4$  [ $\text{M}$ ] $^+$  309.9589, found: 309.9595.

**2,6-Dibromo-4-((2-methyl-5-oxoxazol-4(5H)-ylidene)-methyl)phenyl Acetate.** The title oxazolone (4.04 g, 56%) was prepared from 3,5-dibromo-4-hydroxybenzaldehyde **9m** and obtained as a yellow solid.  $^1\text{H}$  NMR (400 MHz,  $\text{CDCl}_3$ )  $\delta$  2.42 (s, 3H), 2.44 (s, 3H), 6.94 (s, 1H), 8.30 (s, 2H);  $^{13}\text{C}$  NMR (100 MHz,  $\text{CDCl}_3$ )  $\delta$  15.4, 20.1, 117.5, 125.1, 134.0, 134.6, 134.9, 146.6, 166.6, 167.0, 168.4;

HRMS (ESI+)  $m/z$  calcd for  $\text{C}_{13}\text{H}_{10}\text{Br}_2\text{NO}_4$  [ $\text{M} + \text{H}$ ] $^+$  401.8971, found: 401.8990.

**3-(4-Fluorophenyl)-2-hydroxyacrylic Acid (10e).** Acid **10e** (1.48 g, 72%) was obtained from as an orange solid from the corresponding oxazolone **9c**.  $^1\text{H}$  NMR (400 MHz, methanol- $d_4$ ) 6.47 (s, 1H), 7.02 – 7.09 (m, 2H), 7.77 – 7.84 (m, 2H);  $^{13}\text{C}$  NMR (100 MHz, methanol- $d_4$ ) 110.4, 116.0 (d,  $^2J_{\text{C-F}} = 22.2$  Hz), 132.6 (d,  $^3J_{\text{C-F}} = 8.2$  Hz), 132.9, 142.1, 163.3 (d,  $^1J_{\text{C-F}} = 246.3$  Hz), 168.3; HRMS (ESI-)  $m/z$  calcd for  $\text{C}_9\text{H}_6\text{FO}_3$  [ $\text{M} - \text{H}$ ] $^-$  181.0306, found: 181.0296.

**2-Hydroxy-3-(4-(methylthio)phenyl)acrylic Acid (10f).** Acid **10f** (2.05 g, 71%) was obtained as a brown solid from the corresponding oxazolone **9d**.  $^1\text{H}$  NMR (400 MHz, methanol- $d_4$ ) 2.48 (s, 3H), 6.45 (s, 1H), 7.19–7.25 (m, 2H), 7.68 – 7.74 (m, 2H);  $^{13}\text{C}$  NMR (100 MHz, methanol- $d_4$ ) 15.5, 111.2, 127.1, 131.2, 133.2, 139.4, 142.0, 168.3; HRMS (ESI-)  $m/z$  calcd for  $\text{C}_{10}\text{H}_9\text{O}_3\text{S}$  [ $\text{M} - \text{H}$ ] $^-$  209.0278, found: 209.0269.

**2-Hydroxy-3-(3-iodo-4-methoxyphenyl)acrylic Acid (10g).** Acid **10g** (3.25 g, 94%) was obtained as an orange solid from the corresponding oxazolone **9e**.  $^1\text{H}$  NMR (400 MHz, methanol- $d_4$ ) 3.87 (s, 3H), 6.38 (s, 1H), 6.91 (d,  $J = 8.6$  Hz, 1H), 7.70 (dd,  $J = 8.6, 2.0$  Hz, 1H), 8.29 (d,  $J = 2.0$  Hz, 1H);  $^{13}\text{C}$  NMR (100 MHz, DMSO- $d_6$ ) 56.3, 86.0, 108.0, 111.2, 129.6, 130.9, 139.3, 140.8, 156.6, 166.2; HRMS (ESI-)  $m/z$  calcd for  $\text{C}_{10}\text{H}_8\text{IO}_4$  [ $\text{M} - \text{H}$ ] $^-$  318.9473, found: 318.9472.

**3-(3-Bromo-4-fluorophenyl)-2-hydroxyacrylic Acid (10h).** Acid **10h** (1.76 g, 48%) was obtained as a white solid from the corresponding oxazolone **9f**.  $^1\text{H}$  NMR (400 MHz, methanol- $d_4$ ) 6.42 (s, 1H), 7.16 (app-t,  $J = 8.7$  Hz, 1H), 7.66 – 7.72 (m, 1H), 8.14 (dd,  $J = 7.0, 2.1$  Hz, 1H);  $^{13}\text{C}$  NMR (100 MHz, methanol- $d_4$ ) 108.7, 109.5 (d,  $^2J_{\text{C-F}} = 21.5$  Hz), 117.2 (d,  $^2J_{\text{C-F}} = 22.6$  Hz), 131.7 (d,  $^3J_{\text{C-F}} = 6.9$  Hz), 134.6, 135.3, 143.3, 159.2 (d,  $^1J_{\text{C-F}} = 247$  Hz), 167.8; HRMS (ESI-)  $m/z$  calcd for  $\text{C}_9\text{H}_5\text{BrFO}_3$  [ $\text{M} - \text{H}$ ] $^-$  258.9412, found: 258.9418.

**3-(3-Bromo-4-(methylthio)phenyl)-2-hydroxyacrylic Acid (10i).** Acid **10i** (1.88 g, 92%) was obtained as a brown solid from the corresponding oxazolone **9g**.  $^1\text{H}$  NMR (400 MHz, methanol- $d_4$ ) 2.48 (s, 3H), 6.40 (s, 1H), 7.18 (d,  $J = 8.4$  Hz, 1H), 7.66 (dd,  $J = 8.4, 1.8$  Hz), 8.06 (d,  $J = 1.8$  Hz, 1H);  $^{13}\text{C}$  NMR (100 MHz,  $\text{CD}_3\text{OD}/\text{DMSO-}d_6$ ) 15.6, 109.5, 121.9, 126.1, 130.4, 134.1, 134.4, 140.2, 143.1, 167.7; HRMS (ESI-)  $m/z$  calcd for  $\text{C}_{10}\text{H}_8\text{BrO}_3\text{S}$  [ $\text{M} - \text{H}$ ] $^-$  286.9383, found: 286.9379.

**2-Hydroxy-3-(3-iodo-4,5-dimethoxyphenyl)acrylic Acid (10j).** Acid **10j** (2.19 g, 86%) was obtained as a brown solid from the corresponding oxazolone **9h**.  $^1\text{H}$  NMR (400 MHz, methanol- $d_4$ ) 3.78 (s, 3H), 3.85 (s, 3H), 6.37 (s, 1H), 7.48 (d,  $J = 1.7$  Hz, 1H), 7.76 (d,  $J = 1.7$  Hz, 1H);  $^{13}\text{C}$  NMR (100 MHz, methanol- $d_4$ ) 56.4, 60.8, 92.6, 109.7, 115.3, 132.9, 134.8, 142.6, 149.3, 153.5, 168.0; HRMS (ESI-)  $m/z$  calcd for  $\text{C}_{11}\text{H}_{10}\text{IO}_5$  [ $\text{M} - \text{H}$ ] $^-$  348.9578, found: 348.9586.

**3-(3-Bromo-4,5-dimethoxyphenyl)-2-hydroxyacrylic Acid (10k).** Acid **10k** (2.76 g, 93%) was obtained as an orange solid from the corresponding oxazolone **9i**.  $^1\text{H}$  NMR (400 MHz, methanol- $d_4$ ) 3.81 (s, 3H), 3.87 (s, 3H), 6.40 (s, 1H), 7.45 (d,  $J = 1.8$  Hz, 1H), 7.59 (d,  $J = 1.8$  Hz, 1H);  $^{13}\text{C}$  NMR (100 MHz, methanol- $d_4$ ) 56.5, 61.0, 109.8, 114.3, 118.1, 127.0, 134.1, 142.9, 146.7, 154.7, 168.0; HRMS (ESI-)  $m/z$  calcd for  $\text{C}_{11}\text{H}_{10}\text{BrO}_5$  [ $\text{M} - \text{H}$ ] $^-$  300.9717, found: 300.9707.

**3-(3,4-Dimethoxyphenyl)-2-hydroxyacrylic Acid (10l).** Acid **10l** (2.11 g, 62%) was obtained as a brown solid from the corresponding oxazolone **9j**.  $^1\text{H}$  NMR (400 MHz, methanol- $d_4$ ) 3.84 (s, 6H), 6.46 (s, 1H), 6.93 (d,  $J = 8.4$  Hz, 1H), 7.27 (d,  $J = 8.4$  Hz, 1H), 7.57 (s, 1H);  $^{13}\text{C}$  NMR (100 MHz, methanol- $d_4$ ) 56.4 (2C), 112.0, 112.6, 114.4, 124.5, 129.8, 140.9, 150.1, 150.2, 168.6; HRMS (ESI-)  $m/z$  calcd for  $\text{C}_{11}\text{H}_{11}\text{O}_5$  [ $\text{M} - \text{H}$ ] $^-$  223.0612, found: 223.0616.

**2-Hydroxy-3-(3-nitrophenyl)acrylic Acid (10m).** Acid **10m** (1.82 g, 72%) was obtained as a brown solid from the corresponding oxazolone **9k**.  $^1\text{H}$  NMR (400 MHz, methanol- $d_4$ ) 6.56 (s, 1H), 7.56 (app-t,  $J = 8.0$  Hz, 1H), 8.04 (app-d,  $J = 7.9$  Hz, 1H), 8.08 (ddd,  $J = 8.3, 2.4, 0.9$  Hz, 1H), 8.77 (app-t,  $J = 1.9$  Hz, 1H);  $^{13}\text{C}$  NMR (100

MHz, methanol- $d_4$ ) 108.6, 122.6, 124.7, 130.4, 136.4, 138.4, 144.8, 149.8, 167.5; HRMS (ESI<sup>-</sup>)  $m/z$  calcd for  $C_9H_6NO_5$  [ $M - H$ ]<sup>-</sup> 208.0251, found: 208.0251.

**3-(3-Bromo-5-nitrophenyl)-2-hydroxyacrylic Acid (10n).** Acid **10n** (1.68 g, 95%) was obtained as a gray solid from the corresponding oxazolone **9l**. <sup>1</sup>H NMR (400 MHz, methanol- $d_4$ ) 6.49 (s, 1H), 8.19 (app-t,  $J = 1.9$  Hz, 1H), 8.28 (app-t,  $J = 1.4$  Hz, 1H), 8.63 (app-t,  $J = 1.6$  Hz, 1H); <sup>13</sup>C NMR (100 MHz, methanol- $d_4$ ) 15.5, 111.2, 127.1, 127.4, 131.2, 132.1, 133.2, 139.4, 142.0, 168.3; HRMS (ESI<sup>-</sup>)  $m/z$  calcd for  $C_9H_5BrNO_5$  [ $M - H$ ]<sup>-</sup> 285.9357, found: 285.9353.

**3-(3,5-Dibromo-4-hydroxyphenyl)-2-hydroxyacrylic Acid (10o).** Acid **10o** (2.60 g, 82%) was obtained as a brown solid from the corresponding oxazolone **9m**. <sup>1</sup>H NMR (400 MHz, methanol- $d_4$ ) 6.32 (s, 1H), 7.92 (s, 2H); <sup>13</sup>C NMR (100 MHz, CD<sub>3</sub>OD) 108.7, 111.9, 131.1, 134.3, 142.5, 151.3, 167.9; HRMS (ESI<sup>-</sup>)  $m/z$  calcd for  $C_9H_3Br_2O_4$  [ $M - H$ ]<sup>-</sup> 334.8560, found: 334.8560.

**2-Hydroxy-3-(3-methoxy-4-(methylthio)phenyl)acrylic Acid (10p).** Acid **10p** (3.75 g, 98%) was obtained as an off-white solid from the corresponding oxazolone **9n**. <sup>1</sup>H NMR (400 MHz, methanol- $d_4$ ) 2.40 (s, 3H), 3.87 (s, 3H), 6.48 (s, 1H), 7.11 (d,  $J = 8.1$  Hz, 1H), 7.30 (dd,  $J = 8.1, 1.5$  Hz), 7.49 (d,  $J = 1.5$  Hz, 1H); <sup>13</sup>C NMR (100 MHz, CD<sub>3</sub>OD) 14.4, 56.2, 111.6, 112.2, 124.2, 126.2, 128.3, 134.2, 141.9, 157.3, 168.3; HRMS (ESI<sup>-</sup>)  $m/z$  calcd for  $C_{11}H_{11}O_4S$  [ $M - H$ ]<sup>-</sup> 239.0384, found: 239.0370.

**(E)-3-(3-Bromo-4-hydroxyphenyl)-2-(hydroxyimino)-N-(2-methylthioethyl)propanamide (11a).** **11a** (184 mg, 40% from acid **10a**) was obtained as a white solid after flash column chromatography (MeOH:CH<sub>2</sub>Cl<sub>2</sub>, 4: 96) and recrystallization from Et<sub>2</sub>O: mp 102–104 °C.  $R_f$  0.35 (MeOH: CH<sub>2</sub>Cl<sub>2</sub>, 5: 95); IR 3225, 1618, 1548, 1509, 1419, 1013 cm<sup>-1</sup>; <sup>1</sup>H NMR (400 MHz, CD<sub>3</sub>OD)  $\delta$  2.09 (s, 3H), 2.60 (t,  $J = 6.9$  Hz, 2H), 3.44 (t,  $J = 6.9$  Hz, 2H), 3.79 (s, 2H), 6.76 (d,  $J = 8.3$  Hz, 1H), 7.07 (dd,  $J = 8.3, 2.1$  Hz, 1H), 7.37 (d,  $J = 2.1$  Hz, 1H). <sup>13</sup>C NMR (100 MHz, CD<sub>3</sub>OD)  $\delta$  15.2, 28.7, 34.2, 39.6, 110.5, 117.0, 130.4, 130.7, 134.5, 153.2, 153.8, 165.8; HRMS (ESI<sup>+</sup>)  $m/z$  calcd for  $C_{12}H_{14}BrN_2O_3S$  [ $M + H$ ]<sup>+</sup> 347.0060, found: 347.0067. Anal. Calcd for  $C_{12}H_{15}BrN_2O_3S$ : C, 41.51; H, 4.35; N, 8.07. Found: C, 41.45; H, 4.27; N, 7.96.

**(E)-3-(3-Bromo-4-methoxyphenyl)-2-(hydroxyimino)-N-(2-methylthioethyl)propanamide (11b).** **11b** (102 mg, 38% from acid **10b**) was obtained as a yellowish oil after flash column chromatography (AcOEt:PE<sub>40-60</sub>, 1:1).  $R_f$  0.35 (AcOEt:PE<sub>40-60</sub>, 1:1); IR 1658, 1528, 1495, 1257, 1283, 1055 cm<sup>-1</sup>; <sup>1</sup>H NMR (400 MHz, CDCl<sub>3</sub>)  $\delta$  2.10 (s, 3H), 2.65 (t,  $J = 6.4$  Hz, 2H), 3.52 (m, 2H), 3.85 (s, 3H), 3.90 (s, 2H), 6.79 (d,  $J = 8.5$  Hz, 1H), 7.05 (br t, 1H), 7.27 (dd,  $J = 8.5, 2.1$  Hz, 1H), 7.53 (d,  $J = 2.1$  Hz, 1H), 7.69 (br s, 1H). <sup>13</sup>C NMR (100 MHz, CDCl<sub>3</sub>)  $\delta$  15.1, 28.0, 33.6, 37.8, 56.2, 111.4, 111.8, 129.5, 129.7, 134.0, 153.2, 154.5, 162.8; HRMS (ESI<sup>+</sup>)  $m/z$  calcd for  $C_{13}H_{18}BrN_2O_3S$  [ $M + H$ ]<sup>+</sup> 361.0216, found: 361.0222. Anal. Calcd for  $C_{13}H_{17}BrN_2O_3S$ : C, 43.22; H, 4.74; N, 7.75. Found: C, 43.18; H, 4.63; N, 7.78.

**(2E,2'E)-N,N'-(2,2'-Disulfanediy)bis(ethane-2,1-diy)bis(3-(3-bromo-4-methoxyphenyl)-2-(hydroxyimino)propanamide) (11d).** **11d** (185 mg, 49% from acid **10b**) was obtained as a yellow amorphous solid after flash column chromatography (AcOEt:PE<sub>40-60</sub>, 6:4).  $R_f$  0.45 (AcOEt:PE<sub>40-60</sub>, 7:3); IR 1659, 1530, 1495, 1281, 1256, 1055 cm<sup>-1</sup>; <sup>1</sup>H NMR (400 MHz, CDCl<sub>3</sub>)  $\delta$  2.77 (t,  $J = 6.2$  Hz, 4H), 3.59 (m, 4H), 3.81 (s, 6H), 3.87 (s, 4H), 6.74 (d,  $J = 8.5$  Hz, 2H), 7.15 (br t, 2H), 7.24 (dd,  $J = 8.4, 2.1$  Hz, 2H), 7.51 (d,  $J = 2.1$  Hz, 2H). <sup>13</sup>C NMR (100 MHz, CDCl<sub>3</sub>)  $\delta$  28.0, 38.0, 38.3, 56.2, 111.4, 111.8, 129.6, 129.7, 133.9, 152.6, 154.5, 163.5; HRMS (ESI<sup>+</sup>)  $m/z$  calcd for  $C_{24}H_{29}Br_2N_4O_6S_2$  [ $M + H$ ]<sup>+</sup> 690.9890, found: 690.9882. Anal. Calcd for  $C_{24}H_{28}Br_2N_4O_6S_2$ : C, 41.63; H, 4.08; N, 8.09. Found: C, 41.55; H, 4.01; N, 8.15.

**(E)-3-(3-Bromo-4-hydroxyphenyl)-2-(methoxyimino)-N-(2-methylthioethyl)propanamide (11e).** **11e** (98 mg, 43% from acid **10a**) was obtained as a yellow oil after flash column chromatography (AcOEt:PE<sub>40-60</sub>, 1:1).  $R_f$  0.55 (AcOEt:PE<sub>40-60</sub>, 1:1); IR 3327, 1657, 1530, 1509, 1493, 1422, 1045 cm<sup>-1</sup>; <sup>1</sup>H NMR (400 MHz, CDCl<sub>3</sub>)  $\delta$  2.12 (s, 3H), 2.66 (t,  $J = 6.5$  Hz, 2H), 3.52 (m, 2H), 3.81 (s, 2H), 4.01 (s, 3H), 5.46 (br s, 1H), 6.89 (d,  $J = 8.3$  Hz, 1H), 7.06 (br t, 1H), 7.15 (dd,  $J = 8.3, 2.0$  Hz, 1H), 7.40 (d,  $J = 2.0$

Hz, 1H). <sup>13</sup>C NMR (100 MHz, CDCl<sub>3</sub>)  $\delta$  15.2, 28.5, 33.7, 38.0, 63.1, 109.9, 115.9, 129.7, 130.1, 132.5, 150.9, 151.5, 162.5; HRMS (ESI<sup>+</sup>)  $m/z$  calcd for  $C_{13}H_{18}BrN_2O_3S$  [ $M + H$ ]<sup>+</sup> 361.0216, found: 361.0222. Anal. Calcd for  $C_{13}H_{17}BrN_2O_3S$ : C, 43.22; H, 4.74; N, 7.75. Found: C, 43.13; H, 4.72; N, 7.65.

**(2E,2'E)-N,N'-(2,2'-Disulfanediy)bis(ethane-2,1-diy)bis(3-(3-bromo-4-hydroxyphenyl)-2-(methoxyimino)propanamide) (11g).** **11g** (135 mg, 30% from acid **10a**) was obtained as an amorphous yellow solid after purification by flash column chromatography (AcOEt:PE<sub>40-60</sub>, 5.8:4:0.2).  $R_f$  0.6 (AcOEt:PE<sub>40-60</sub>, 7:3); IR 3356, 1657, 1528, 1508, 1492, 1422, 1045 cm<sup>-1</sup>; <sup>1</sup>H NMR (400 MHz, CDCl<sub>3</sub>)  $\delta$  2.81 (t,  $J = 6.4$  Hz, 4H), 3.61 (m, 4H), 3.81 (s, 4H), 4.00 (s, 6H), 5.56 (br s, 2H), 6.88 (d,  $J = 8.3$  Hz, 2H), 7.06 (br t, 2H), 7.14 (dd,  $J = 8.3, 2.0$  Hz, 2H), 7.39 (d,  $J = 2.0$  Hz, 2H). <sup>13</sup>C NMR (100 MHz, CDCl<sub>3</sub>)  $\delta$  28.5, 37.6, 38.3, 63.1, 110.0, 115.9, 129.7, 130.2, 132.5, 150.9, 151.5, 162.6; HRMS (ESI<sup>+</sup>)  $m/z$  calcd for  $C_{24}H_{29}Br_2N_4O_6S_2$  [ $M + H$ ]<sup>+</sup> 690.9890, found: 690.9893. Anal. Calcd for  $C_{24}H_{28}Br_2N_4O_6S_2$ : C, 41.63; H, 4.08; N, 8.09. Found: C, 41.56; H, 3.97; N, 8.15.

**(2E,2'E)-N,N'-(2,2'-Disulfanediy)bis(ethane-2,1-diy)bis(3-(3-bromo-4-methoxyphenyl)-2-(methoxyimino)propanamide) (11h).** **11h** (161 mg, 41% from acid **10b**) was obtained as a white solid after purification by flash column chromatography (AcOEt:PE<sub>40-60</sub>, 1:1) and recrystallization (AcOEt/hexane): mp 81–83 °C (AcOEt/hexane);  $R_f$  0.5 (AcOEt:PE<sub>40-60</sub>, 1:1); **11h** has been reported previously,<sup>23-25</sup> <sup>1</sup>H NMR (400 MHz, CDCl<sub>3</sub>)  $\delta$  2.82 (t,  $J = 6.4$  Hz, 4H), 3.62 (m, 4H), 3.82 (s, 4H), 3.84 (s, 6H), 4.00 (s, 6H), 6.78 (d,  $J = 8.4$  Hz, 2H), 7.06 (br t, 2H), 7.20 (dd,  $J = 8.4, 2.2$  Hz, 2H), 7.46 (d,  $J = 2.2$  Hz, 2H); HRMS (ESI<sup>+</sup>)  $m/z$  calcd for  $C_{26}H_{33}Br_2N_4O_6S_2$  [ $M + H$ ]<sup>+</sup> 719.0203, found: 719.0209.

**(2E,2'E)-N,N'-(2,2'-Disulfanediy)bis(ethane-2,1-diy)bis(2-(hydroxyimino)-3-phenylpropanamide) (11i).** **11i** (225 mg, 24% from acid **10c**) was obtained as an amorphous white solid after purification by flash column chromatography (gradient acetone:PE<sub>40-60</sub>, 3:7 to 4:6) and precipitation from CH<sub>2</sub>Cl<sub>2</sub>.  $R_f$  0.3 (acetone:PE<sub>40-60</sub>, 3:7); IR (neat) 1654, 1625, 1522, 1493, 1426, 1000 cm<sup>-1</sup>; <sup>1</sup>H NMR (400 MHz, CD<sub>3</sub>OD)  $\delta$  2.79 (t,  $J = 6.7$  Hz, 4H), 3.50 (t,  $J = 6.7$  Hz, 4H), 3.91 (s, 4H), 7.10–7.16 (m, 2H), 7.17–7.30 (m, 8H). <sup>13</sup>C NMR (100 MHz, CD<sub>3</sub>OD)  $\delta$  30.0, 38.5, 39.6, 127.3, 129.4, 130.1, 138.2, 153.3, 166.0; HRMS (ESI<sup>+</sup>)  $m/z$  calcd for  $C_{22}H_{27}N_4O_4S_2$  [ $M + H$ ]<sup>+</sup> 475.1468, found: 475.1470. Anal. Calcd for  $C_{22}H_{26}N_4O_4S_2$ : C, 55.68; H, 5.52; N, 11.81. Found: C, 55.75; H, 5.44; N, 11.89.

**(2E,2'E)-N,N'-(2,2'-Disulfanediy)bis(ethane-2,1-diy)bis(2-(hydroxyimino)-3-(4-hydroxyphenyl)propanamide) (11j).** **11j** (175 mg, 20% from acid **10d**) was obtained as an amorphous white solid after purification by flash column chromatography (gradient acetone:PE<sub>40-60</sub>, 4:6 to 1:1). Important degradation was observed during the final deprotection step for reaction times superior to 2 h. Only partial conversion to the product (and recovery of the starting material) was achieved during the deprotection step, avoiding degradation and allowing efficient purification of the product.  $R_f$  0.3 (acetone:PE<sub>40-60</sub>, 1:1); IR (neat) 1655, 1613, 1531, 1511, 1437, 1214, 1011, 980 cm<sup>-1</sup>; <sup>1</sup>H NMR (400 MHz, CD<sub>3</sub>OD)  $\delta$  2.79 (t,  $J = 6.8$  Hz, 4H), 3.51 (t,  $J = 6.8$  Hz, 4H), 3.80 (s, 4H), 6.62–6.67 (m, 4H), 7.05–7.11 (m, 4H). <sup>13</sup>C NMR (100 MHz, CD<sub>3</sub>OD)  $\delta$  29.1, 38.5, 39.6, 116.1, 128.9, 131.2, 153.8, 156.9, 166.2; HRMS (ESI<sup>+</sup>)  $m/z$  calcd for  $C_{22}H_{27}N_4O_6S_2$  [ $M + H$ ]<sup>+</sup> 507.1367, found: 507.1371. Anal. Calcd for  $C_{22}H_{26}N_4O_6S_2$ : C, 52.16; H, 5.17; N, 11.06. Found: C, 52.10; H, 5.11; N, 10.97.

**(2E,2'E)-N,N'-(2,2'-Disulfanediy)bis(ethane-2,1-diy)bis(3-(4-fluorophenyl)-2-(hydroxyimino)propanamide) (11k).** **11k** (225 mg, 29% from acid **10e**) was obtained as an amorphous white solid after purification by flash column chromatography (gradient acetone:PE<sub>40-60</sub>, 3:7 to 4:6).  $R_f$  0.25 (acetone:PE<sub>40-60</sub>, 3:7); IR (neat) 1654, 1625, 1528, 1508, 1427, 1235, 1221, 1023, 1001 cm<sup>-1</sup>; <sup>1</sup>H NMR (400 MHz, CD<sub>3</sub>OD)  $\delta$  2.81 (t,  $J = 6.6$  Hz, 4H), 3.52 (t,  $J = 6.6$  Hz, 4H), 3.88 (s, 4H), 6.89–7.00 (m, 4H), 7.23–7.33 (m, 4H). <sup>13</sup>C NMR (100 MHz, CD<sub>3</sub>OD)  $\delta$  29.2, 38.6, 39.6, 115.9 (d,  $J_{CF} = 21.4$  Hz), 131.8 (d,  $J_{CF} = 7.5$  Hz), 134.1, 153.1, 162.9 (d,  $J_{CF} = 243$  Hz),

165.9; HRMS (ESI+)  $m/z$  calcd for  $C_{22}H_{25}F_2N_4O_4S_2$  [ $M + H$ ]<sup>+</sup> 511.1280, found: 511.1269. Anal. Calcd for  $C_{22}H_{24}F_2N_4O_4S_2$ : C, 51.75; H, 4.74; N, 10.97. Found: C, 51.73; H, 4.64; N, 10.92.

**(2*E*,2'*E*)-*N,N'*-(2,2'-Disulfanediyldis(ethane-2,1-diyl))bis(2-(hydroxyimino)-3-(4-(methylthio)phenyl)propanamide) (11l).** **11l** (114 mg, 20% from acid **10f**) was obtained as an amorphous light yellow solid after purification by flash column chromatography (acetone:PE<sub>40-60</sub>: 3:7 then MeOH:CH<sub>2</sub>Cl<sub>2</sub> 1:9).  $R_f$  0.4 (acetone:PE<sub>40-60</sub>: 4:6); IR (neat) 1653, 1625, 1523, 1492, 1424, 1000  $cm^{-1}$ ; <sup>1</sup>H NMR (400 MHz, DMSO-*d*<sub>6</sub>)  $\delta$  2.42 (s, 6H), 2.81 (t,  $J = 6.7$  Hz, 4H), 3.41 (m, 4H), 3.76 (s, 4H), 7.15 (m, 8H), 8.06 (br t,  $J = 5.4$ , 2H), 11.85 (s, 2H). <sup>13</sup>C NMR (100 MHz, DMSO-*d*<sub>6</sub>)  $\delta$  14.9, 28.3, 36.9, 38.1, 126.1, 129.3, 133.5, 135.4, 151.6, 163.2; HRMS (ESI+)  $m/z$  calcd for  $C_{24}H_{31}N_4O_4S_4$  [ $M + H$ ]<sup>+</sup> 567.1223, found: 567.1230. Anal. Calcd for  $C_{24}H_{30}N_4O_4S_4$ : C, 50.86; H, 5.34; N, 9.89. Found: C, 50.91; H, 5.30; N, 9.81.

**(2*E*,2'*E*)-*N,N'*-(2,2'-Disulfanediyldis(ethane-2,1-diyl))bis(2-(hydroxyimino)-3-(3-iodo-4-methoxyphenyl)propanamide) (11m).** **11m** (428 mg, 36% from acid **10g**) was obtained as an amorphous light yellow solid after purification by flash column chromatography (gradient acetone:PE<sub>40-60</sub>: 3:7 to 4:6).  $R_f$  0.45 (acetone:PE<sub>40-60</sub>: 4:6); IR (neat) 1657, 1624, 1527, 1487, 1437, 1279, 1251, 1047, 1014, 981  $cm^{-1}$ ; <sup>1</sup>H NMR (400 MHz, CD<sub>3</sub>OD)  $\delta$  2.80 (t,  $J = 6.7$  Hz, 4H), 3.50 (t,  $J = 6.7$  Hz, 4H), 3.79 (s, 6H), 3.81 (s, 4H), 6.79 (d,  $J = 8.5$  Hz, 2H), 7.24 (dd,  $J = 8.5$ , 2.2 Hz, 2H), 7.67 (d,  $J = 2.2$  Hz, 2H). <sup>13</sup>C NMR (100 MHz, CD<sub>3</sub>OD)  $\delta$  28.6, 38.7, 39.6, 56.9, 86.2, 112.0, 131.5, 132.3, 141.0, 153.1, 158.3, 165.9; HRMS (ESI+)  $m/z$  calcd for  $C_{24}H_{29}I_2N_4O_6S_2$  [ $M + H$ ]<sup>+</sup> 786.9612, found: 786.9631. Anal. Calcd for  $C_{24}H_{28}I_2N_4O_6S_2$ : C, 36.65; H, 3.59; N, 7.12. Found: C, 36.73; H, 3.48; N, 7.07.

**(2*E*,2'*E*)-*N,N'*-(2,2'-Disulfanediyldis(ethane-2,1-diyl))bis(3-(3-bromo-4-fluorophenyl)-2-(hydroxyimino)propanamide) (11n).** **11n** (201 mg, 30% from acid **10h**) was obtained as an amorphous white solid after purification by flash column chromatography (gradient acetone:PE<sub>40-60</sub>: 3:7 to 4:6).  $R_f$  0.55 (acetone:PE<sub>40-60</sub>: 4:6); IR (neat) 1655, 1623, 1528, 1491, 1427, 1404, 1242, 1358, 1013, 984  $cm^{-1}$ ; <sup>1</sup>H NMR (400 MHz, CD<sub>3</sub>OD)  $\delta$  2.82 (t,  $J = 6.7$  Hz, 4H), 3.53 (t,  $J = 6.7$  Hz, 4H), 3.87 (s, 4H), 7.06 (app-t,  $J = 8.6$  Hz, 2H), 7.27 (ddd,  $J = 8.4$ , 4.7, 2.2 Hz, 2H), 7.51 (dd,  $J = 6.7$ , 2.2 Hz, 2H). <sup>13</sup>C NMR (100 MHz, CD<sub>3</sub>OD)  $\delta$  29.0, 38.6, 39.6, 109.2 (d,  $J_{CF} = 21.1$  Hz), 117.2 (d,  $J_{CF} = 22.5$  Hz), 131.2 (d,  $J_{CF} = 6.9$  Hz), 135.1, 136.1 (d,  $J_{CF} = 3.5$  Hz), 152.5, 159.1 (d,  $J_{CF} = 245$  Hz), 165.7; HRMS (ESI+)  $m/z$  calcd for  $C_{22}H_{23}Br_2F_2N_4O_4S_2$  [ $M + H$ ]<sup>+</sup> 666.9490, found: 666.9500. Anal. Calcd for  $C_{22}H_{22}Br_2F_2N_4O_4S_2$ : C, 39.53; H, 3.32; N, 8.38. Found: C, 39.58; H, 3.30; N, 8.28.

**(2*E*,2'*E*)-*N,N'*-(2,2'-Disulfanediyldis(ethane-2,1-diyl))bis(3-(3-bromo-4-(methylthio)phenyl)-2-(hydroxyimino)propanamide) (11o).** **11o** (270 mg, 25% from acid **10i**) was obtained as an amorphous light yellow solid after purification by flash column chromatography (gradient acetone:PE<sub>40-60</sub>: 3:7 to 1:1).  $R_f$  0.25 (acetone:PE<sub>40-60</sub>: 3:7); IR (neat) 1655, 1623, 1526, 1462, 1432, 1026  $cm^{-1}$ ; <sup>1</sup>H NMR (400 MHz, CD<sub>3</sub>OD)  $\delta$  2.41 (s, 6H), 2.80 (t,  $J = 6.7$  Hz, 4H), 3.51 (t,  $J = 6.7$  Hz, 4H), 3.85 (s, 4H), 7.09 (d,  $J = 8.2$  Hz, 2H), 7.25 (dd,  $J = 8.2$ , 1.8 Hz, 2H), 7.45 (d,  $J = 1.8$  Hz, 2H). <sup>13</sup>C NMR (100 MHz, CD<sub>3</sub>OD)  $\delta$  15.8, 29.1, 38.7, 39.6, 122.4, 126.8, 130.1, 134.2, 136.3, 138.9, 152.7, 165.8; HRMS (ESI+)  $m/z$  calcd for  $C_{24}H_{29}Br_2N_4O_4S_4$  [ $M + H$ ]<sup>+</sup> 722.9433, found: 722.9441. Anal. Calcd for  $C_{24}H_{28}Br_2N_4O_4S_4$ : C, 39.78; H, 3.90; N, 7.73. Found: C, 39.73; H, 3.85; N, 7.67.

**(2*E*,2'*E*)-*N,N'*-(2,2'-Disulfanediyldis(ethane-2,1-diyl))bis(2-(hydroxyimino)-3-(3-iodo-4,5-dimethoxyphenyl)propanamide) (11p).** **11p** (295 mg, 23% from acid **10j**) was obtained as an amorphous light yellow solid after purification by flash column chromatography (gradient acetone:PE<sub>40-60</sub>: 3:7 to 4:6).  $R_f$  0.15 (acetone:PE<sub>40-60</sub>: 3:7); IR (neat) 1657, 1528, 1480, 1413, 1268, 1137, 1041, 993  $cm^{-1}$ ; <sup>1</sup>H NMR (400 MHz, CD<sub>3</sub>OD)  $\delta$  2.82 (t,  $J = 6.7$  Hz, 4H), 3.51 (t,  $J = 6.7$  Hz, 4H), 3.71 (s, 6H), 3.80 (s, 6H), 3.83 (s, 4H), 6.95 (d,  $J = 1.7$  Hz, 2H), 7.23 (d,  $J = 1.7$  Hz, 2H). <sup>13</sup>C NMR (100 MHz, CD<sub>3</sub>OD)  $\delta$  29.2, 38.7, 39.6, 56.4, 60.8, 92.5, 115.3, 131.9, 136.5, 148.7, 152.8, 153.7, 165.8; HRMS (ESI+)  $m/z$  calcd for  $C_{26}H_{33}I_2N_4O_8S_2$  [ $M + H$ ]<sup>+</sup> 846.9824, found: 846.9858. Anal. Calcd for

$C_{26}H_{32}I_2N_4O_8S_2$ : C, 36.89; H, 3.81; N, 6.62. Found: C, 36.92; H, 3.79; N, 6.57.

**(2*E*,2'*E*)-*N,N'*-(2,2'-Disulfanediyldis(ethane-2,1-diyl))bis(3-(3-bromo-4,5-dimethoxyphenyl)-2-(hydroxyimino)propanamide) (11q).** **11q** (339 mg, 45% from acid **10k**) was obtained as an amorphous white solid after purification by flash column chromatography (gradient acetone:PE<sub>40-60</sub>: 3:7 to 4:6).  $R_f$  0.35 (acetone:PE<sub>40-60</sub>: 4:6); IR (neat) 1656, 1625, 1528, 1487, 1413, 1271, 1138, 1044, 998  $cm^{-1}$ ; <sup>1</sup>H NMR (400 MHz, CD<sub>3</sub>OD)  $\delta$  2.82 (t,  $J = 6.7$  Hz, 4H), 3.52 (t,  $J = 6.7$  Hz, 4H), 3.74 (s, 6H), 3.81 (s, 6H), 3.85 (s, 4H), 6.93 (d,  $J = 1.8$  Hz, 2H), 7.03 (d,  $J = 1.8$  Hz, 2H). <sup>13</sup>C NMR (100 MHz, CD<sub>3</sub>OD)  $\delta$  29.5, 38.7, 39.6, 56.6, 60.9, 114.3, 118.0, 126.1, 135.7, 146.1, 152.7, 154.8, 165.8; HRMS (ESI+)  $m/z$  calcd for  $C_{26}H_{33}Br_2N_4O_8S_2$  [ $M + H$ ]<sup>+</sup> 751.0101, found: 751.0117. Anal. Calcd for  $C_{26}H_{32}Br_2N_4O_8S_2$ : C, 41.50; H, 4.29; N, 7.45. Found: C, 41.45; H, 4.21; N, 7.48.

**(2*E*,2'*E*)-*N,N'*-(2,2'-Disulfanediyldis(ethane-2,1-diyl))bis(3-(3,4-dimethoxyphenyl)-2-(hydroxyimino)propanamide) (11r).** **11r** (115 mg, 13% from acid **10l**) was obtained as an amorphous light yellow solid after purification by flash column chromatography (gradient acetone:PE<sub>40-60</sub>: 3:7 to 4:6). Important degradation was observed during the final deprotection step for reaction times superior to 2 h. Only partial conversion to the product (and recovery of the starting material) was achieved during the deprotection step, avoiding degradation and allowing efficient purification of the product.  $R_f$  0.25 (acetone:PE<sub>40-60</sub>: 4:6); IR (neat) 1658, 1628, 1511, 1419, 1259, 1233, 1141, 1022  $cm^{-1}$ ; <sup>1</sup>H NMR (400 MHz, CD<sub>3</sub>OD)  $\delta$  2.79 (t,  $J = 6.7$  Hz, 4H), 3.50 (t,  $J = 6.7$  Hz, 4H), 3.76 (s, 6H), 3.77 (s, 6H), 3.85 (s, 4H), 6.76–6.84 (m, 4H), 6.90 (d,  $J = 1.5$  Hz, 2H). <sup>13</sup>C NMR (100 MHz, CD<sub>3</sub>OD)  $\delta$  29.5, 38.7, 39.6, 56.4, 56.6, 113.1, 114.3, 122.7, 131.0, 149.1, 150.3, 153.5, 166.1; HRMS (ESI+)  $m/z$  calcd for  $C_{26}H_{35}N_4O_8S_2$  [ $M + H$ ]<sup>+</sup> 595.1891, found: 595.1897. Anal. Calcd for  $C_{26}H_{34}N_4O_8S_2$ : C, 52.51; H, 5.76; N, 9.42. Found: C, 52.54; H, 5.72; N, 9.49.

**(2*E*,2'*E*)-*N,N'*-(2,2'-Disulfanediyldis(ethane-2,1-diyl))bis(3-(3-bromo-5-nitrophenyl)-2-(hydroxyimino)propanamide) (11t).** **11t** (123 mg, 11% from acid **10n**) was obtained as an amorphous white solid after purification by flash column chromatography (gradient acetone:PE<sub>40-60</sub>: 3:7 to 4:6).  $R_f$  0.25 (acetone:PE<sub>40-60</sub>: 3:7); IR (neat) 1655, 1620, 1526, 1426, 1344, 1026, 988  $cm^{-1}$ ; <sup>1</sup>H NMR (400 MHz, CD<sub>3</sub>OD)  $\delta$  2.83 (t,  $J = 6.7$  Hz, 4H), 3.53 (t,  $J = 6.7$  Hz, 4H), 4.02 (s, 4H), 7.84–7.87 (m, 2H), 8.12–8.15 (m, 2H), 8.20 (m, 2H). <sup>13</sup>C NMR (100 MHz, CD<sub>3</sub>OD–DMSO-*d*<sub>6</sub>)  $\delta$  29.8, 38.7, 39.6, 123.3, 124.1, 125.5, 139.4, 142.8, 150.2, 151.7, 165.0; HRMS (ESI+)  $m/z$  calcd for  $C_{22}H_{23}Br_2N_6O_8S_2$  [ $M + H$ ]<sup>+</sup> 720.9380, found: 720.9412. Anal. Calcd for  $C_{22}H_{22}Br_2N_6O_8S_2$ : C, 36.58; H, 3.07; N, 11.63. Found: C, 36.64; H, 3.01; N, 11.68.

**(2*E*,2'*E*)-*N,N'*-(2,2'-Disulfanediyldis(ethane-2,1-diyl))bis(3-(3,5-dibromo-4-hydroxyphenyl)-2-(hydroxyimino)propanamide) (11u).** **11u** (270 mg, 22% from acid **10o**) was obtained as an amorphous light yellow solid after purification by flash column chromatography (gradient acetone:PE<sub>40-60</sub>: 35:65 to 50:50).  $R_f$  0.3 (acetone:PE<sub>40-60</sub>: 4:6); IR (neat) 1653, 1625, 1520, 1544, 1474, 1406, 1159  $cm^{-1}$ ; <sup>1</sup>H NMR (400 MHz, CD<sub>3</sub>OD)  $\delta$  2.82 (t,  $J = 6.7$  Hz, 4H), 3.53 (t,  $J = 6.7$  Hz, 4H), 3.79 (s, 4H), 7.39 (s, 4H). <sup>13</sup>C NMR (100 MHz, CD<sub>3</sub>OD)  $\delta$  28.5, 38.6, 39.6, 112.0, 132.3, 134.0, 150.7, 152.6, 165.7; HRMS (ESI+)  $m/z$  calcd for  $C_{22}H_{23}Br_2N_4O_6S_2$  [ $M + H$ ]<sup>+</sup> 818.7787, found: 818.7811. Anal. Calcd for  $C_{22}H_{22}Br_2N_4O_6S_2$ : C, 32.14; H, 2.70; N, 6.81. Found: C, 32.08; H, 2.70; N, 6.74.

**(2*E*,2'*E*)-*N,N'*-(Hexane-1,6-diyl)bis(3-(3-bromo-4-hydroxyphenyl)-2-(hydroxyimino)propanamide) (11w).** **11w** (44 mg) was obtained in 12% yield from acid **10a** and hexane-1,6-diamine **16**, after purification by flash column chromatography (AcOEt:PE<sub>40-60</sub>). Amorphous white solid; **11w** has been previously reported in the literature<sup>35</sup> and our data matched reported ones.  $R_f$  0.1 (AcOEt:PE<sub>40-60</sub>: 1:1); <sup>1</sup>H NMR (400 MHz, CD<sub>3</sub>OD)  $\delta$  1.22–1.32 (m, 4H), 1.42–1.52 (m, 4H), 3.20 (t,  $J = 7.0$  Hz, 4H), 3.79 (s, 4H), 6.76 (d,  $J = 8.3$  Hz, 2H), 7.06 (dd,  $J = 8.3$ , 2.1 Hz, 2H), 7.36 (d,  $J = 2.1$  Hz, 2H). <sup>13</sup>C NMR (100 MHz, CD<sub>3</sub>OD)  $\delta$  27.5, 28.8, 30.4, 40.2, 110.5, 117.1, 130.4, 130.7, 134.5, 153.6, 153.8, 165.8; HRMS (ESI+)  $m/z$  calcd for  $C_{24}H_{29}Br_2N_4O_6$  [ $M + H$ ]<sup>+</sup> 627.0448, found: 627.0470.

(*E*)-3-(3-Bromo-4-hydroxyphenyl)-*N*-(3-(2-((*E*)-3-(3-bromo-4-hydroxyphenyl)-2-(hydroxyimino)propanamido)ethylthio)propyl)-2-(hydroxyimino)propanamide (**11x**). **11x** (53 mg) was obtained in 14% yield from acid **10a** and 3-(2-aminoethylthio)propan-1-amine **15**,<sup>65</sup> after purification by flash column chromatography (AcOEt:PE<sub>40-60</sub>). Amorphous white solid; *R*<sub>f</sub> 0.1 (AcOEt:PE<sub>40-60</sub> 1:1); IR (neat) 3248, 1646, 1605, 1539, 1495, 1420 cm<sup>-1</sup>; <sup>1</sup>H NMR (400 MHz, CD<sub>3</sub>OD) δ 1.74 (q, *J* = 7.2 Hz, 2H), 2.50 (t, *J* = 7.2 Hz, 2H), 2.61 (t, *J* = 6.7 Hz, 2H), 3.30 (t, *J* = 7.2 Hz, 2H), 3.39 (t, *J* = 6.7 Hz, 2H), 3.79 (s, 4H), 6.76 (d, *J* = 8.3 Hz, 2H), 7.06 (dd, *J* = 8.3, 2.1 Hz, 2H), 7.36 (d, *J* = 2.1 Hz, 2H). <sup>13</sup>C NMR (100 MHz, CD<sub>3</sub>OD) δ 28.7, 28.8, 29.9, 30.4, 32.1, 39.4, 40.0, 110.5 (2C), 117.1 (2C), 130.4 (2C), 130.7 (2C), 134.5 (2C), 153.2, 153.5, 153.8 (2C), 165.8, 166.0; HRMS (ESI+) *m/z* calcd for C<sub>23</sub>H<sub>27</sub>Br<sub>2</sub>N<sub>4</sub>O<sub>6</sub>S [M + H]<sup>+</sup> 645.0013, found: 645.0045. Anal. Calcd for C<sub>23</sub>H<sub>26</sub>Br<sub>2</sub>N<sub>4</sub>O<sub>6</sub>S: C, 42.74; H, 4.05; N, 8.67. Found: C, 42.89; H, 3.98; N, 8.53.

**General Procedure for the Synthesis of Ketoamide-Containing Analogues 17a–d.** The appropriate crude acid (1 equiv) was added to a solution of the appropriate primary amine (1 equiv for 2-(methylthio)ethanamine, 0.5 equiv for cystamine, obtained from neutralization of cystamine dihydrochloride with sodium hydroxide in water and extraction with chloroform) and diisopropylethylamine (1.1 equiv) at 0 °C in THF, followed by py-BOP (1.1 equiv). The resulting mixture was stirred overnight at rt. The following day the solvent was evaporated in vacuo and the product purified by flash column chromatography without any prior workup.

3-(3-Bromo-4-hydroxyphenyl)-*N*-(2-(methylthio)ethyl)-2-oxopropanamide (**17a**). Following the general procedure described above, crude acid **10a** was coupled with 2-(methylthio)ethanamine **13** to afford product **17a** (370 mg, 40%) as a white solid after purification by flash column chromatography (AcOEt:CH<sub>2</sub>Cl<sub>2</sub>, 1:9) and recrystallization from Et<sub>2</sub>O: mp 55–59 °C; *R*<sub>f</sub> 0.6 (AcOEt:PE<sub>40-60</sub>, 1:1); IR 3346, 1655, 1543, 1505, 1419 cm<sup>-1</sup>; <sup>1</sup>H NMR (400 MHz, CDCl<sub>3</sub>) δ 2.12 (s, 3H), 2.66 (t, *J* = 6.5 Hz, 2H), 3.52 (m, 2H), 4.13 (s, 2H), 5.47 (br s, 1H), 6.98 (d, *J* = 8.3 Hz, 1H), 7.11 (dd, *J* = 8.3, 2.0 Hz, 1H), 7.26 (br t, 1H), 7.37 (d, *J* = 2.0 Hz, 1H). <sup>13</sup>C NMR (100 MHz, CDCl<sub>3</sub>) δ 15.1, 33.4, 37.8, 41.8, 110.3, 116.2, 126.0, 130.7, 133.1, 151.5, 159.8, 195.3; HRMS (ESI+) *m/z* calcd for C<sub>12</sub>H<sub>15</sub>BrNO<sub>3</sub>S [M + H]<sup>+</sup> 331.9951, found: 331.9945. Anal. Calcd for C<sub>12</sub>H<sub>14</sub>BrNO<sub>3</sub>S: C, 43.38; H, 4.25; N, 4.22. Found: C, 43.48; H, 4.16; N, 4.13.

3-(3-Bromo-4-methoxyphenyl)-*N*-(2-(methylthio)ethyl)-2-oxopropanamide (**17b**). According to the general procedure described above, crude acid **10b** was coupled with 2-(methylthio)ethanamine **13** to afford product **17b** (481 mg, 63%) as a white solid after purification by flash column chromatography (AcOEt:PE<sub>40-60</sub>, 4:6) and recrystallization from Bu<sub>2</sub>O: mp 64–66 °C; *R*<sub>f</sub> 0.65 (AcOEt:PE<sub>40-60</sub>, 1:1); IR 1682, 1521, 1498, 1281, 1257, 1055 cm<sup>-1</sup>; <sup>1</sup>H NMR (400 MHz, CDCl<sub>3</sub>) δ 2.12 (s, 3H), 2.66 (t, *J* = 6.5 Hz, 2H), 3.52 (m, 2H), 3.88 (s, 3H), 4.13 (s, 2H), 6.86 (d, *J* = 8.4 Hz, 1H), 7.17 (dd, *J* = 8.4, 2.1 Hz, 1H), 7.26 (br t, 1H), 7.44 (d, *J* = 2.1 Hz, 1H). <sup>13</sup>C NMR (100 MHz, CDCl<sub>3</sub>) δ 15.1, 33.4, 37.8, 41.8, 56.2, 111.7, 112.0, 126.0, 130.0, 134.5, 155.1, 159.8, 195.4; HRMS (ESI+) *m/z* calcd for C<sub>13</sub>H<sub>17</sub>BrNO<sub>3</sub>S [M + H]<sup>+</sup> 346.0107, found: 346.0111. Anal. Calcd for C<sub>13</sub>H<sub>16</sub>BrNO<sub>3</sub>S: C, 45.10; H, 4.66; N, 4.05. Found: C, 45.19; H, 4.60; N, 3.92.

*N,N'*-(2,2'-Disulfanediy)bis(ethane-2,1-diyl)bis(3-(3-bromo-4-hydroxyphenyl)-2-oxopropanamide) (**17c**). According to the general procedure described above, crude acid **10a** was coupled with cystamine **14** to afford product **17c** (117 mg, 24%) as an amorphous white solid after purification by flash column chromatography (AcOEt:CH<sub>2</sub>Cl<sub>2</sub>, 3:7). *R*<sub>f</sub> 0.6 (AcOEt:CH<sub>2</sub>Cl<sub>2</sub>, 4:6); IR 3354, 1668, 1495, 1418 cm<sup>-1</sup>; <sup>1</sup>H NMR (400 MHz, CDCl<sub>3</sub>) δ 2.82 (t, *J* = 6.4 Hz, 4H), 3.63 (m, 4H), 4.12 (s, 4H), 5.49 (br s, 2H), 6.97 (d, *J* = 8.3 Hz, 2H), 7.10 (dd, *J* = 8.3, 2.0 Hz, 2H), 7.30 (br t, 2H), 7.37 (d, *J* = 2.0 Hz, 2H). <sup>13</sup>C NMR (100 MHz, CDCl<sub>3</sub>) δ 37.2, 38.4, 41.8, 110.3, 116.2, 125.9, 130.7, 133.1, 151.6, 160.0, 195.3; HRMS (ESI+) *m/z* calcd for C<sub>22</sub>H<sub>23</sub>Br<sub>2</sub>N<sub>2</sub>O<sub>6</sub>S<sub>2</sub> [M + H]<sup>+</sup> 632.9359, found: 632.9368. Anal. Calcd for C<sub>22</sub>H<sub>22</sub>Br<sub>2</sub>N<sub>2</sub>O<sub>6</sub>S<sub>2</sub>: C, 41.65; H, 3.50; N, 4.42. Found: C, 41.54; H, 3.58; N, 4.37.

*N,N'*-(2,2'-Disulfanediy)bis(ethane-2,1-diyl)bis(3-(3-bromo-4-methoxyphenyl)-2-oxopropanamide) (**17d**). According to the general procedure described above, crude acid **10b** was coupled with

cystamine **14** to afford product **17d** (255 mg, 42%) as an amorphous white solid after purification by flash column chromatography (AcOEt:PE<sub>40-60</sub>, 6:4). *R*<sub>f</sub> 0.4 (AcOEt:PE<sub>40-60</sub>, 1:1); IR 1660, 1526, 1496, 1256 cm<sup>-1</sup>; <sup>1</sup>H NMR (400 MHz, CDCl<sub>3</sub>) δ 2.83 (t, *J* = 6.4 Hz, 4H), 3.63 (m, 4H), 3.87 (s, 6H), 4.13 (s, 4H), 6.85 (d, *J* = 8.5 Hz, 2H), 7.16 (dd, *J* = 8.4, 2.2 Hz, 2H), 7.31 (br t, 2H), 7.43 (d, *J* = 2.2 Hz, 2H). <sup>13</sup>C NMR (100 MHz, CDCl<sub>3</sub>) δ 37.2, 38.4, 41.8, 56.2, 111.7, 112.0, 125.9, 130.0, 134.5, 155.1, 160.0, 195.3; HRMS (ESI+) *m/z* calcd for C<sub>24</sub>H<sub>27</sub>Br<sub>2</sub>N<sub>2</sub>O<sub>6</sub>S<sub>2</sub> [M + H]<sup>+</sup> 660.9672, found: 660.9692. Anal. Calcd for C<sub>24</sub>H<sub>26</sub>Br<sub>2</sub>N<sub>2</sub>O<sub>6</sub>S<sub>2</sub>: C, 43.52; H, 3.96; N, 4.23. Found: C, 43.62; H, 3.88; N, 4.10.

(*E*)-3-(3-Bromo-4-hydroxyphenyl)-2-hydrazono-*N*-(2-(methylthio)ethyl)propanamide (**18a**). To a solution of compound **17a** (365 mg, 1.10 mmol, 1 equiv) in freshly distilled methanol (11 mL) at rt was added hydrazine monohydrate (59 μL, 1.21 mmol, 1.1 equiv). The resulting mixture was heated to reflux for 2.5 h and then cooled to room temperature. The solvent was then evaporated in vacuo and the product (220 mg, 58%) obtained as a white solid after purification by flash column chromatography (AcOEt/CH<sub>2</sub>Cl<sub>2</sub>, 15:85) and recrystallization from CH<sub>2</sub>Cl<sub>2</sub>: mp 103–104 °C (CH<sub>2</sub>Cl<sub>2</sub>); *R*<sub>f</sub> 0.25 (AcOEt:CH<sub>2</sub>Cl<sub>2</sub>, 1:9); IR 3414, 3359, 3116, 1633, 1620, 1528, 1509, 1421 cm<sup>-1</sup>; <sup>1</sup>H NMR (400 MHz, CDCl<sub>3</sub>) δ 2.14 (s, 3H), 2.69 (t, *J* = 6.5 Hz, 2H), 3.56 (m, 2H), 3.81 (s, 2H), 5.59 (br s, 1H), 5.68 (br s, 2H), 6.92 (d, *J* = 8.3 Hz, 1H), 7.07 (dd, *J* = 8.3, 2.0 Hz, 1H), 7.31 (d, *J* = 2.0 Hz, 1H), 7.32 (br t, 1H). <sup>13</sup>C NMR (100 MHz, CDCl<sub>3</sub>) δ 15.2, 27.6, 34.0, 37.9, 110.6, 116.4, 128.8, 129.2, 131.5, 141.6, 151.2, 164.6; HRMS (ESI+) *m/z* calcd for C<sub>12</sub>H<sub>17</sub>BrN<sub>3</sub>O<sub>2</sub>S [M + H]<sup>+</sup> 346.0219, found: 346.0214. Anal. Calcd for C<sub>12</sub>H<sub>16</sub>BrN<sub>3</sub>O<sub>2</sub>S: C, 41.63; H, 4.66; N, 12.14. Found: C, 41.55; H, 4.60; N, 12.07.

**Crystal data for 18a.** C<sub>12</sub>H<sub>16</sub>BrN<sub>3</sub>O<sub>2</sub>S, *M* = 346.25, monoclinic, *P*2<sub>1</sub>/*c* (no. 14), *a* = 10.18411(14), *b* = 14.96067(18), *c* = 9.13052(13) Å, β = 99.2862(14)°, *V* = 1372.91(3) Å<sup>3</sup>, *Z* = 4, *D*<sub>c</sub> = 1.675 g cm<sup>-3</sup>, μ(Mo *K*α) = 3.148 mm<sup>-1</sup>, *T* = 173 K, colorless plate-like needles, Oxford Diffraction Xcalibur 3 diffractometer; 4603 independent measured reflections (*R*<sub>int</sub> = 0.0222), *F*<sup>2</sup> refinement, *R*<sub>1</sub>(obs) = 0.0240, *wR*<sub>2</sub>(all) = 0.0532, 3319 independent observed absorption-corrected reflections [*I*<sub>h</sub> > 4σ(*I*<sub>h</sub>)], 2θ<sub>max</sub> = 65°, 188 parameters. CCDC 804665.

(*E*)-3-(3-Bromo-4-methoxyphenyl)-2-hydrazono-*N*-(2-(methylthio)ethyl)propanamide (**18b**). To a solution of compound **17b** (380 mg, 1.10 mmol, 1 equiv) in freshly distilled methanol (11 mL) at rt was added hydrazine monohydrate (59 μL, 1.21 mmol, 1.1 equiv). The resulting mixture was heated to reflux for 2.5 h and then cooled to room temperature. The solvent was then evaporated in vacuo and the product (273 mg, 69%) obtained as an amorphous white solid after purification by flash column chromatography (AcOEt/CH<sub>2</sub>Cl<sub>2</sub>, 1:9). *R*<sub>f</sub> 0.55 (AcOEt:CH<sub>2</sub>Cl<sub>2</sub>, 1:9); IR 3376, 3338, 1637, 1517, 1491, 1251, 1051 cm<sup>-1</sup>; <sup>1</sup>H NMR (400 MHz, CDCl<sub>3</sub>) δ 2.14 (s, 3H), 2.69 (t, *J* = 6.5 Hz, 2H), 3.56 (m, 2H), 3.82 (s, 2H), 3.86 (s, 3H), 5.67 (br s, 2H), 6.81 (d, *J* = 8.4 Hz, 1H), 7.13 (dd, *J* = 8.4, 2.1 Hz, 1H), 7.31 (br t, 1H), 7.40 (d, *J* = 2.1 Hz, 1H). <sup>13</sup>C NMR (100 MHz, CDCl<sub>3</sub>) δ 15.2, 27.6, 34.0, 37.9, 56.3, 112.1, 112.3, 128.3, 128.8, 133.0, 141.7, 154.7, 164.5; HRMS (ESI+) *m/z* calcd for C<sub>13</sub>H<sub>19</sub>BrN<sub>3</sub>O<sub>2</sub>S [M + H]<sup>+</sup> 360.0376, found: 360.0372. Anal. Calcd for C<sub>13</sub>H<sub>18</sub>BrN<sub>3</sub>O<sub>2</sub>S: C, 43.34; H, 5.04; N, 11.66. Found: C, 43.26; H, 4.93; N, 11.56.

(2*E*,2'*E*)-*N,N'*-(2,2'-Disulfanediy)bis(ethane-2,1-diyl)bis(3-(3-bromo-4-hydroxyphenyl)-2-hydrazonopropanamide) (**18c**). To a solution of compound **17c** (235 mg, 0.35 mmol, 1 equiv) in freshly distilled methanol (3.6 mL) at rt was added hydrazine monohydrate (38 μL, 0.78 mmol, 2.2 equiv). The resulting mixture was heated to reflux for 2.5 h and then cooled to room temperature. The solvent was then evaporated in vacuo and the product (182 mg, 74%) obtained as an amorphous white solid after purification by flash column chromatography (MeOH/CH<sub>2</sub>Cl<sub>2</sub>, 6:94). *R*<sub>f</sub> 0.35 (MeOH:CH<sub>2</sub>Cl<sub>2</sub>, 6:94); IR 3359, 3312, 1626, 1530, 1503, 1193 cm<sup>-1</sup>; <sup>1</sup>H NMR (400 MHz, DMSO-*d*<sub>6</sub>) δ 2.82 (t, *J* = 6.8 Hz, 4H), 3.42 (m, 4H), 3.64 (s, 4H), 6.81 (d, *J* = 8.3 Hz, 2H), 7.01 (dd, *J* = 8.3, 1.9 Hz, 2H), 7.21 (s, 4H), 7.31 (d, *J* = 1.9 Hz, 2H), 7.79 (t, *J* = 5.9 Hz, 2H), 9.97 (s, 2H). <sup>13</sup>C NMR (100 MHz, DMSO-*d*<sub>6</sub>) 26.1, 37.3, 38.0,

108.8, 116.0, 128.7, 129.0, 132.4, 136.8, 152.1, 165.0; HRMS (ESI+)  $m/z$  calcd for  $C_{22}H_{27}Br_2N_3O_4S_2$  [ $M + H$ ]<sup>+</sup> 660.9896, found: 660.9910. Anal. Calcd for  $C_{22}H_{26}Br_2N_3O_4S_2$ : C, 39.89; H, 3.96; N, 12.69. Found: C, 39.84; H, 3.88; N, 12.61.

**(2*E*,2'*E*)-*N,N'*-(2,2'-Disulfanediylbis(ethane-2,1-diyl))bis(3-(3-bromo-4-methoxyphenyl)-2-hydranonopropanamide) (18d).** To a solution of compound 17d (350 mg, 0.53 mmol, 1 equiv) in freshly distilled methanol (5.3 mL) at rt was added hydrazine monohydrate (57  $\mu$ L, 1.16 mmol, 1 equiv). The resulting mixture was heated to reflux for 2.5 h and then cooled to room temperature. The solvent was then evaporated in vacuo and the product (217 mg, 59%) obtained as an amorphous white solid after purification by flash column chromatography (MeOH/CH<sub>2</sub>Cl<sub>2</sub> 2:98).  $R_f$  0.3 (AcOEt:PE<sub>40-60</sub> 3:7); IR 3396, 3316, 1637, 1516, 1493, 1253, 1053 cm<sup>-1</sup>; <sup>1</sup>H NMR (400 MHz, CD<sub>3</sub>OD)  $\delta$  2.87 (t,  $J = 6.7$  Hz, 4H), 3.56 (t,  $J = 6.7$  Hz, 4H), 3.76 (s, 4H), 3.81 (s, 6H), 6.90 (d,  $J = 8.4$  Hz, 2H), 7.16 (dd,  $J = 8.4, 2.0$  Hz, 2H), 7.39 (d,  $J = 2.0$  Hz, 2H). <sup>13</sup>C NMR (100 MHz, CD<sub>3</sub>OD)  $\delta$  27.7, 39.1, 39.6, 56.8, 112.5, 113.4, 129.8, 131.3, 134.1, 139.2, 156.0, 167.8; HRMS (ESI+)  $m/z$  calcd for  $C_{24}H_{31}Br_2N_6O_4S_2$  [ $M + H$ ]<sup>+</sup> 689.0209, found: 689.0206. Anal. Calcd for  $C_{24}H_{30}Br_2N_6O_4S_2$ : C, 41.75; H, 4.38; N, 12.17. Found: C, 41.81; H, 4.30; N, 12.12.

***N,N'*-(2,2'-Disulfanediylbis(ethane-2,1-diyl))bis(3-(3-bromo-4-hydroxyphenyl)propanamide) (23).** To a solution of cystamine (43.5 mg, 0.286 mmol, 1 equiv), triethylamine (239  $\mu$ L, 1.71 mmol, 6 equiv), and HOBt (92.6 mg, 0.685 mmol, 2.4 equiv) in DCM (10 mL), under an argon atmosphere, at rt, were added successively EDCI (131 mg, 0.685 mmol, 2.4 equiv) and 3-(3-bromo-4-hydroxyphenyl)propanoic acid 22 (140 mg, 0.571 mmol, 2 equiv). The resulting mixture was stirred for 15 h at rt before the solvent was evaporated. The residue was then dissolved in ethyl acetate (10 mL) and washed with 1 N aqueous HCl (5 mL), saturated aqueous NaHCO<sub>3</sub> (5 mL), and brine (5 mL). The organic phase was dried (MgSO<sub>4</sub>) and concentrated. The product (83 mg, 48%) was obtained as a white solid after purification by flash column chromatography (AcOEt).  $R_f$  0.2 (AcOEt). IR (neat) 3283, 1635, 1537, 1506, 1495, 1419, 1221 cm<sup>-1</sup>; <sup>1</sup>H NMR (400 MHz, CD<sub>3</sub>OD)  $\delta$  2.43 (t,  $J = 7.4$  Hz, 4H), 2.70 (t,  $J = 6.7$  Hz, 4H), 2.81 (t,  $J = 7.4$  Hz, 4H), 3.42 (t,  $J = 6.7$  Hz, 4H), 6.79 (d,  $J = 8.3$  Hz, 2H), 6.99 (dd,  $J = 8.3, 2.1$  Hz, 2H), 7.30 (d,  $J = 2.1$  Hz, 2H). <sup>13</sup>C NMR (100 MHz, CD<sub>3</sub>OD)  $\delta$  31.6, 38.5, 38.9, 39.5, 110.7, 117.2, 129.7, 133.9, 134.7, 153.7, 175.2; HRMS (ESI+)  $m/z$  calcd for  $C_{22}H_{27}Br_2N_2O_4S_2$  [ $M + H$ ]<sup>+</sup> 604.9774, found: 604.9781. Anal. Calcd for  $C_{22}H_{26}Br_2N_2O_4S_2$ : C, 43.58; H, 4.32; N, 4.62. Found: C, 43.66; H, 4.38; N, 4.71.

**3-(1,3-Dioxoisindolin-2-yl)-*N*-(tetrahydro-2*H*-pyran-2-yloxy)propanamide (31).** To a mixture of 3-(1,3-dioxoisindolin-2-yl)propanoic acid 29<sup>42</sup> (3.5 g, 16.0 mmol, 1 equiv) and *O*-(tetrahydro-2*H*-pyran-2-yl)hydroxylamine<sup>37</sup> (1.96 g, 16.8 mmol, 1.05 equiv) in chloroform (135 mL) was added EDCI (3.37 g, 17.6 mmol, 1.1 equiv), followed by DMAP (195 mg, 1.60 mmol, 0.1 equiv). The resulting mixture was stirred overnight at rt. The day after, the reaction mixture was concentrated and water (195 mL) was added and extracted with AcOEt (3  $\times$  135 mL). The combined organic layers were washed with brine (195 mL), dried (Na<sub>2</sub>SO<sub>4</sub>), and concentrated in vacuo. The product (4.06 g, 80%) was obtained as a white solid after purification by flash column chromatography (gradient MeOH/CH<sub>2</sub>Cl<sub>2</sub> 2:98 to 10:90).  $R_f$  0.45 (AcOEt:CH<sub>2</sub>Cl<sub>2</sub> 1:1); IR (neat) 1710, 1680, 1653, 1398, 1113 cm<sup>-1</sup>; <sup>1</sup>H NMR (400 MHz, DMSO-*d*<sub>6</sub>)  $\delta$  1.38–1.72 (m, 6H), 2.36 (t,  $J = 7.0$  Hz, 2H), 3.40 (m, 1H), 3.78 (t,  $J = 7.0$  Hz, 2H), 3.83 (m, 1H), 4.74 (m, 1H), 7.81–7.91 (m, 4H), 11.08 (s, 1H). <sup>13</sup>C NMR (100 MHz, DMSO-*d*<sub>6</sub>)  $\delta$  18.3, 24.5, 27.6, 31.1, 34.0, 61.3, 100.7, 122.9, 131.6, 134.2, 166.2, 167.5; HRMS (ESI+)  $m/z$  calcd for  $C_{16}H_{18}N_2NaO_5$  [ $M + Na$ ]<sup>+</sup> 341.1108, found: 341.1109. Anal. Calcd for  $C_{16}H_{18}N_2O_5$ : C, 60.37; H, 5.70; N, 8.80. Found: C, 60.31; H, 5.62; N, 8.75.

**4-(1,3-Dioxoisindolin-2-yl)-*N*-(tetrahydro-2*H*-pyran-2-yloxy)butanamide (32).** To a mixture of 4-(1,3-dioxoisindolin-2-yl)butanoic acid 30<sup>42</sup> (4.0 g, 17.2 mmol, 1 equiv) and *O*-(tetrahydro-2*H*-pyran-2-yl)hydroxylamine<sup>37</sup> (2.11 g, 18.0 mmol, 1.05 equiv) in chloroform (145 mL) was added EDCI (3.62 g, 18.9 mmol, 1.1 equiv)

followed by DMAP (210 mg, 1.72 mmol, 0.1 equiv). The resulting mixture was stirred overnight at rt. The day after, the reaction mixture was concentrated and water (210 mL) was added and extracted with CHCl<sub>3</sub> (3  $\times$  140 mL). The combined organic layers were washed with brine (210 mL), dried (Na<sub>2</sub>SO<sub>4</sub>), and concentrated in vacuo. The product (5.35 g, 94%) was obtained as a white solid after purification by flash column chromatography (MeOH/CH<sub>2</sub>Cl<sub>2</sub> 5:95).  $R_f$  0.45 (AcOEt:CH<sub>2</sub>Cl<sub>2</sub> 1:1); <sup>1</sup>H NMR (400 MHz, DMSO-*d*<sub>6</sub>)  $\delta$  1.40–1.70 (m, 6H), 1.81 (app quintuplet,  $J = 7.2$  Hz, 2H), 2.03 (t,  $J = 7.2$  Hz, 2H), 3.47 (m, 1H), 3.57 (t,  $J = 6.9$  Hz, 2H), 3.88 (m, 1H), 4.75 (m, 1H), 7.78–7.92 (m, 4H), 10.92 (s, 1H). <sup>13</sup>C NMR (100 MHz, DMSO-*d*<sub>6</sub>)  $\delta$  18.2, 23.8, 24.6, 27.7, 29.6, 37.0, 61.2, 100.8, 122.9, 131.6, 134.2, 167.8, 168.2. HRMS (ESI+)  $m/z$  calcd for  $C_{17}H_{20}N_2NaO_5$  [ $M + Na$ ]<sup>+</sup> 355.1264, found: 355.1266. Anal. Calcd for  $C_{17}H_{20}N_2O_5$ : C, 61.44; H, 6.07; N, 8.43. Found: C, 61.51; H, 6.02; N, 8.36.

**3-Amino-*N*-(tetrahydro-2*H*-pyran-2-yloxy)propanamide (33).** To a mixture of 3-(1,3-dioxoisindolin-2-yl)-*N*-(tetrahydro-2*H*-pyran-2-yloxy)propanamide 31 (3.23 g, 10.1 mmol, 1 equiv) in freshly distilled methanol (65 mL) was added hydrazine monohydrate (517  $\mu$ L, 10.7 mmol, 1.05 equiv). The resulting mixture was heated to reflux for 2.5 h and then cooled to rt. The white precipitate formed was filtered off and washed with a small amount of methanol. The methanolic phase was concentrated in vacuo, and the product (805 mg, 42%) was obtained as a white solid after purification by flash column chromatography (CHCl<sub>3</sub>/MeOH/aq NH<sub>3</sub> 80:18:2) without prior workup.  $R_f$  0.2 (CHCl<sub>3</sub>/MeOH/aq NH<sub>3</sub> 80:18:2); IR (neat) 1659, 1573, 1361, 1112, 1073, 1031 cm<sup>-1</sup>; <sup>1</sup>H NMR (400 MHz, DMSO-*d*<sub>6</sub>)  $\delta$  1.42–1.74 (m, 6H), 2.06 (t,  $J = 6.6$  Hz, 2H), 2.72 (t,  $J = 6.6$  Hz, 2H), 3.44–3.54 (m, 1H), 3.85–3.96 (m, 1H), 4.52 (br s, 2H), 4.81 (m, 1H). <sup>13</sup>C NMR (100 MHz, DMSO-*d*<sub>6</sub>)  $\delta$  18.2, 24.6, 27.7, 36.3, 38.1, 61.2, 100.7, 168.3; HRMS (ESI+)  $m/z$  calcd for  $C_8H_{17}N_2O_3$  [ $M + H$ ]<sup>+</sup> 189.1234, found: 189.1232. Anal. Calcd for  $C_8H_{16}N_2O_3$ : C, 51.05; H, 8.57; N, 14.88. Found: C, 51.15; H, 8.65; N, 14.94.

**4-Amino-*N*-(tetrahydro-2*H*-pyran-2-yloxy)butanamide (34).** To a mixture of 4-(1,3-dioxoisindolin-2-yl)-*N*-(tetrahydro-2*H*-pyran-2-yloxy)butanamide 32 (2.50 g, 7.52 mmol, 1 equiv) in freshly distilled methanol (50 mL) was added hydrazine monohydrate (401  $\mu$ L, 8.27 mmol, 1.1 equiv). The resulting mixture was stirred overnight at rt. The white precipitate formed was filtered off and washed with a small amount of methanol. The methanolic phase was concentrated in vacuo, and the product (758 mg, 50%) was obtained as a white solid after purification by flash column chromatography (CHCl<sub>3</sub>/MeOH/aq NH<sub>3</sub> 80:18:2) without prior workup.  $R_f$  0.2 (CHCl<sub>3</sub>/MeOH/aq NH<sub>3</sub> 80:18:2); <sup>1</sup>H NMR (400 MHz, DMSO-*d*<sub>6</sub>)  $\delta$  1.42–1.74 (m, 8H), 2.00 (t,  $J = 7.3$  Hz, 2H), 2.49 (t,  $J = 7.3$  Hz, 2H), 3.44–3.54 (m, 1H), 3.85–3.96 (m, 1H), 4.56 (br s, 2H), 4.79 (m, 1H). <sup>13</sup>C NMR (100 MHz, DMSO-*d*<sub>6</sub>)  $\delta$  18.2, 24.6, 27.7, 29.0, 29.8, 41.0, 61.2, 100.7, 169.1; HRMS (ESI+)  $m/z$  calcd for  $C_9H_{19}N_2O_3$  [ $M + H$ ]<sup>+</sup> 203.1390, found: 203.1389. Anal. Calcd for  $C_9H_{18}N_2O_3$ : C, 53.45; H, 8.97; N, 13.85. Found: C, 53.53; H, 8.90; N, 13.81.

**(*E*)-3-(3-Bromo-4-hydroxyphenyl)-*N*-(3-(hydroxyamino)-3-oxopropyl)-2-(hydroxyimino)propanamide (24).** To a solution of acid 10a (1 equiv) in freshly distilled pyridine (2 mL/mmol), under argon, was added *O*-(tetrahydro-2*H*-pyran-2-yl)hydroxylamine 12 (1.5 equiv). The resulting mixture was stirred overnight at room temperature. Pyridine was then removed in vacuo, and the residue was dissolved in 1 N HCl (5.5 mL/mmol) and extracted three times with ethyl acetate (5.5 mL/mmol). The combined organic layers were dried (Na<sub>2</sub>SO<sub>4</sub>), filtered, and concentrated to afford the crude *O*-THP-protected oxime intermediate, used for the next step without further purification. To a solution of the crude *O*-THP-protected oxime intermediate (1 equiv) in dry dioxane (2.7 mL/mmol) under argon were added EDCI (1.7 equiv) and NHS (1.9 equiv). The resulting mixture was stirred at room temperature for 3 h. The solvent was then evaporated in vacuo. The residue was dissolved in EtOAc (12 mL/mmol) and washed with saturated aqueous NaHCO<sub>3</sub> (2  $\times$  12 mL/mmol), 1 N aqueous HCl (2  $\times$  12 mL/mmol), and brine (1  $\times$  12 mL/mmol). The organic phase was then dried (Na<sub>2</sub>SO<sub>4</sub>) and filtered, and

the solvent was evaporated in vacuo. The residue was dissolved in dry dioxane (2.7 mL/mmol) under argon, and a second solution of 3-amino-*N*-(tetrahydro-2*H*-pyran-2-yloxy)propanamide **33** (1.0 equiv) and NEt<sub>3</sub> (1.0 equiv) in dry dioxane (2.7 mL/mmol) were added. The resulting mixture was then stirred overnight at rt. The next day the solvent was evaporated and the product was purified by flash column chromatography (1:1 AcOEt/PE<sub>40–60</sub>). The *O*-THP-diprotected precursor was then dissolved in an anhydrous 0.5 M solution of HCl in 9:1 dioxane/*i*PrOH (21 mL/mmol). The resulting mixture was stirred at rt and the reaction monitored by TLC. After 20 h, the solvent was evaporated in vacuo and the product (81 mg, 13%) was obtained as a white solid after purification by flash column chromatography (1:9 MeOH/DCM). *R*<sub>f</sub> 0.15 (MeOH:CH<sub>2</sub>Cl<sub>2</sub>, 1:9); IR (neat) 3202, 1626, 1532, 1492, 1418, 1211, 993 cm<sup>-1</sup>; <sup>1</sup>H NMR (400 MHz, DMSO-*d*<sub>6</sub>) δ 2.17 (t, *J* = 7.1 Hz, 2H), 3.32 (app-q, *J* = 7.0 Hz, 2H), 3.67 (s, 2H), 6.83 (d, *J* = 8.3 Hz, 1H), 7.01 (dd, *J* = 8.3, 2.0 Hz, 1H), 7.29 (d, *J* = 2.0 Hz, 1H), 7.93 (t, *J* = 5.8 Hz, 1H), 8.74 (s, 1H), 10.03 (s, 1H), 10.44 (s, 1H), 11.87 (s, 1H). <sup>13</sup>C NMR (100 MHz, DMSO-*d*<sub>6</sub>) δ 27.5, 31.9, 35.4, 108.8, 116.1, 128.7, 129.0, 132.7, 151.6, 152.3, 162.8, 167.3; HRMS (ESI+) *m/z* calcd for C<sub>12</sub>H<sub>15</sub>BrN<sub>3</sub>O<sub>5</sub> [M + H]<sup>+</sup> 360.0190, found: 360.0195. Anal. Calcd for C<sub>12</sub>H<sub>15</sub>BrN<sub>3</sub>O<sub>5</sub>: C, 40.02; H, 3.92; N, 11.67. Found: C, 40.14; H, 3.83; N, 11.61.

**(E)-4-(3-(3-Bromo-4-hydroxyphenyl)-2-(hydroxyimino)propanamido)-*N*-hydroxybutanamide (25).** To a solution of acid **10a** (1 equiv) in freshly distilled pyridine (2 mL/mmol), under argon, was added *O*-(tetrahydro-2*H*-pyran-2-yl)hydroxylamine **12** (1.5 equiv). The resulting mixture was stirred overnight at room temperature. Pyridine was then removed in vacuo, and the residue was dissolved in 1 N HCl (5.5 mL/mmol) and extracted three times with ethyl acetate (5.5 mL/mmol). The combined organic layers were dried (Na<sub>2</sub>SO<sub>4</sub>), filtered, and concentrated to afford the crude *O*-THP-protected oxime intermediate, used for the next step without further purification. To a solution of the crude *O*-THP-protected oxime intermediate (1 equiv) in dry dioxane (2.7 mL/mmol) under argon were added EDCI (1.7 equiv) and NHS (1.9 equiv). The resulting mixture was stirred at room temperature for 3 h. The solvent was then evaporated in vacuo. The residue was dissolved in EtOAc (12 mL/mmol) and washed with saturated aqueous NaHCO<sub>3</sub> (2 × 12 mL/mmol), 1 N aqueous HCl (2 × 12 mL/mmol), and brine (1 × 12 mL/mmol). The organic phase was then dried (Na<sub>2</sub>SO<sub>4</sub>), filtered, and the solvent evaporated in vacuo. The residue was dissolved in dry dioxane (2.7 mL/mmol) under argon, and a second solution of 4-amino-*N*-(tetrahydro-2*H*-pyran-2-yloxy)butanamide **34** (1.0 equiv) and NEt<sub>3</sub> (1.0 equiv) in dry dioxane (2.7 mL/mmol) were added. The resulting mixture was then stirred overnight at rt. The day after the solvent was evaporated, and the product was purified by flash column chromatography (1:1 acetone/PE<sub>40–60</sub>). The *O*-THP-diprotected precursor was then dissolved in an anhydrous 0.5 M solution of HCl in 9:1 dioxane/*i*PrOH (21 mL/mmol). The resulting mixture was stirred at rt and the reaction monitored by TLC. After 20 h, the solvent was evaporated in vacuo and the product (170 mg, 15%) was obtained as a white solid after purification by flash column chromatography (1:9 MeOH/DCM). *R*<sub>f</sub> 0.15 (MeOH:CH<sub>2</sub>Cl<sub>2</sub>, 1:9); IR (neat) 3184, 1623, 1536, 1493, 1418, 1208, 993 cm<sup>-1</sup>; <sup>1</sup>H NMR (400 MHz, DMSO-*d*<sub>6</sub>) δ 1.63 (app-quintuplet, *J* = 7.3 Hz, 2H), 1.92 (t, *J* = 7.3 Hz, 2H), 3.11 (m, 2H), 3.68 (s, 2H), 6.83 (d, *J* = 8.3 Hz, 1H), 7.01 (dd, *J* = 8.3, 2.0 Hz, 1H), 7.29 (d, *J* = 2.0 Hz, 1H), 8.00 (t, *J* = 6.0 Hz, 1H), 8.67 (s, 1H), 10.03 (s, 1H), 10.34 (s, 1H), 11.77 (s, 1H). <sup>13</sup>C NMR (100 MHz, DMSO-*d*<sub>6</sub>) δ 25.2, 27.7, 29.8, 38.3, 108.7, 116.0, 128.8, 129.0, 132.7, 151.9, 152.2, 163.1, 168.7; HRMS (ESI+) *m/z* calcd for C<sub>13</sub>H<sub>17</sub>BrN<sub>3</sub>O<sub>5</sub> [M + H]<sup>+</sup> 374.0346, found: 374.0359. Anal. Calcd for C<sub>13</sub>H<sub>16</sub>BrN<sub>3</sub>O<sub>5</sub>: C, 41.73; H, 4.31; N, 11.23. Found: C, 41.63; H, 4.23; N, 11.18.

#### General Procedure 1 for the in Situ Reduction of Disulfides.

To the appropriate dimeric compound (neat, 1.0 equiv) was added solid TCEP (1.5 equiv). Dilution with the adequate amount of a 9:1 DMSO/distilled water solution and agitation for 20–30 min (magnetic stirrer) at rt afforded the required stock solution of thiol. All thiols were used immediately after reduction.

Example: preparation of a 50 mM stock solution of **11c**. To pure **11c** (5.0 mg, 1 equiv) was added solid TCEP (3.2 mg, 1.5 equiv). A 301 μL amount of a 9:1 DMSO/water was added, and the resulting mixture was stirred for 20 min at rt. The resulting stock solution was used immediately. Complete and clean reduction was observed by <sup>1</sup>H NMR (see Supporting Information). MS (see Supporting Information) allowed for the observation of [M – H]<sup>-</sup>, [M + HCOO]<sup>-</sup>, and [2M – H]<sup>-</sup> ions.

#### General Procedure 2 for the in Situ Reduction of Disulfides.

A 18.75 mM solution (S1) of TCEP in a 9:1 (v/v) mixture of DMSO/deionized water was prepared. To 40 μL of S1 was added 10 μL of a 50 mM solution (S2) of the appropriate dimeric compound. The resulting mixture was incubated for 20 min at 25 °C in the dark, with occasional shaking. The resulting 20 mM stock solution of thiol was used immediately.

**HDAC Assay.** DMSO, Pluronic, TCEP, and trypsin (bovine pancreas) were purchased from Sigma-Aldrich and Boc-Lys(Ac)-AMC from Bachem (Switzerland). The recombinant human histone deacetylases HDAC1 and HDAC6 were obtained from BPS Bioscience (US). All reactions were performed in black half-area 96-well microplates (Greiner bio-one, Germany) according to the general procedure described by Wegener et al.<sup>43</sup> with some minor modifications. The reaction buffer contains 50 mM KH<sub>2</sub>PO<sub>4</sub>/K<sub>2</sub>HPO<sub>4</sub>, 15 mM Tris/HCl, pH 8, 250 mM NaCl, 0.001% (v/v) Pluronic, and 250 μM EDTA. The buffer components were purchased from Merck (Germany), Roth (Germany), and Sigma-Aldrich.

The fluorogenic HDAC assay consists of two steps: In the first step the Boc-Lys(Ac)-AMC substrate is deacetylated by the corresponding HDAC. The deacetylated substrate, therefore containing a basic amino acid residue, serves as substrate for trypsin in the subsequent second step. The second step generates the signal due to the release of fluorescent AMC, whose fluorescence serves as an indirect measure of HDAC enzyme activity. Stock solutions (50 mM) of test compounds were prepared in DMSO and diluted for testing using reaction buffer.

Thiols were obtained from their corresponding disulfides via general procedures described in the Experimental Section. Varying the procedure did not show significant influence on the final calculated IC<sub>50</sub>. Test experiments have shown TCEP to have no influence on enzyme activity at concentrations up to 25 μM.

A serial dilution of test compounds was preincubated with 7.4 nM HDAC1 or 2.8 nM HDAC6, respectively, for 20 min at 21 ± 1 °C in the dark. The enzyme reaction was initiated by the addition of Boc-Lys(Ac)-AMC substrate. The reaction mixture was incubated at 30 °C in the dark and stopped after 60 min by the addition of a mixture of 67 μM trypsin and 200 nM SAHA. The fluorescence of AMC serves as an indirect measure of HDAC enzyme activity. The kinetics of AMC release was measured on a PolarStar fluorescence plate reader (BMG) using an excitation wavelength of 340 nm and an emission wavelength of 460 nm. Complete cleavage of deacetylated Boc-Lys-AMC by trypsin was achieved after about 10–15 min. The fluorescence intensity of the plateau was averaged over at least 5 min and normalized with respect to percent of enzyme activity. Finally, the normalized fluorescence intensities were plotted versus the concentration of test compounds and fitted to a four-parameter logistic model<sup>66</sup> to calculate the IC<sub>50</sub> values.

**Protein Expression and Purification of Histone Deacetylase-like Amidohydrolase (HDAH).** The recombinant HDAH from *Bordetella* strain FB188 (DSM 11172) containing an N-terminal His6-affinity tag was prepared as previously reported.<sup>44</sup> Briefly, HDAH was expressed in *E. coli* strain BL21, and the cell lysate was applied to a His-Trap FF (Amersham Biosciences) column loaded with zinc ions. After removal of nonbinding proteins, the pure enzyme was eluted with 500 mM imidazole. The resulting pure enzyme was dialyzed against assay buffer and directly used to test compounds. The purity of HDAH (>98%) was determined using polyacrylamide gel electrophoresis and Coomassie Brilliant Blue G-250 to stain protein.

**DNMT Assay.** All reactions were performed in 384-well microtiter plates (Corning, catalogue #3575, UK). The end-point detection reaction was carried out using the restriction endonuclease Glal purchased from SybEnzyme (Novosibirsk, Russia). The break light



hemimethylated oligonucleotide used was obtained from ATDBio Ltd. (Southampton, UK) (5'-FAM-ATCTAGCGSATCAGTTTCT-GATGSGSTAGAT-dab 3'). S-(5'-Adenosyl)-L-methionine chloride (SAM), methyl donor for the DNMT1 reaction, was obtained from Sigma (Gillingham, UK), SAH, S-(5'-adenosyl)-L-homocysteine, and all other reagents were also obtained from Sigma unless otherwise stated. The final fluorescent signal was read using a BMG-LabTech Pherastar (Aylesbury, UK) at 520 nm (Em)/485 nm (Ex) wavelengths. All single point data were analyzed using Excel, and dose-response curves were analyzed and IC<sub>50</sub> values calculated using XLfit 4.0 (IDBS, Guilford, UK). DNMT1 enzyme (from a baculovirus expression system) was a kind gift from CRT, London. All assay reagents were added to the assay plates using a multidropCombi (ThermoScientific, Basingstoke, UK), all compound dilutions were performed using a BeckmanCoulter Biomek FX (High Wycombe, UK) for the serial dilutions, and a PlateMatePlus (ThermoScientific-Matrix, Basingstoke, UK) for all plate to plate transfer dilutions and compound additions to assay plates.

All assays were carried out as follows: into the wells of a 384-well plate was added 1  $\mu$ L of compound (at the appropriate concentration for testing, normally 30  $\mu$ M for single-point screening) and then a 5  $\mu$ L mix of SAM (10  $\mu$ M final concentration) and hemimethylated oligo (125 nM final concentration). The reaction was started by the addition of 5  $\mu$ L of DNMT1 enzyme at 80 nM final concentration in DNMT assay buffer (40 mM MOPS, 25 mM NaCl, 0.5 mM MgCl<sub>2</sub>, pH 6.5, Triton X-100 0.01%, and 1 mM DTT). Negative control wells were prepared as above, but no SAM was added to mimic a complete inhibition of the DNMT1 reaction. For the positive control wells, no compounds were added. The reaction was incubated for 1 h at room temperature. The reaction was stopped and signal developed by the addition of a 40  $\mu$ L mix of a Glu1 0.00156U/ $\mu$ L and SAH, 125  $\mu$ M final concentration mix in Glu1 buffer (Tris-HCl 40 mM, NaCl 80 mM, MgCl<sub>2</sub> 0.75 mM, Triton X-100 0.01%, and 1 mM DTT, pH 8). This second enzymatic reaction was incubated for 7 h at room temperature prior to reading the fluorescence signal at 520 nm. Thiols were obtained from their respective disulfides according to the general procedures described in the Experimental Section.

**M.SssI in Vitro DNA Methylation Assay.** Enzyme reagents for the M.SssI in vitro DNA methylation studies were obtained from New England Biolabs. One unit of M.SssI enzyme was incubated with 1  $\mu$ g of bacteriophage  $\lambda$  DNA in a 20  $\mu$ L reaction volume containing 50 mM NaCl, 10 mM Tris-HCl (pH 7.9 at 25 °C), 10 mM MgCl<sub>2</sub>, 1 mM dithiothreitol (NEBuffer2), and 160  $\mu$ M S-adenosylmethionine, in the presence and absence inhibitors for 2 h at 37 °C. Following DNA methylation, the M.SssI enzyme was heat inactivated by incubation at 65 °C for 20 min. The extent of DNA methylation was subsequently assessed by the addition of 30  $\mu$ L of NEBuffer 2 containing 10 units of BstI restriction endonuclease and digestion for 1 h at 60 °C. The digested DNA was analyzed by gel electrophoresis using a 1.5% agarose gel.

**Cell Lines.** Human cancer cell lines, breast (MCF7), lung (A549), and normal human lung fibroblast lines (WI-38) were all purchased from American Type Cell Culture (ATCC). MCF7 and A549 cells were maintained in Dulbecco's Modified Eagle's Medium (DMEM) supplemented with 10% fetal bovine serum (Invitrogen, UK), 2 mM L-glutamine (Invitrogen, Netherlands), and 1X Non Essential Amino Acids (Fisher Scientific). WI38 cells were maintained in Minimum Essential Medium Eagle (MEM) supplemented with 10% fetal bovine serum and 2 mM L-glutamine. Cells were routinely passaged and maintained at 37 °C, 5% CO<sub>2</sub>.

**Sulphorhodamine B Assay.** Short-term growth inhibition was measured using the SRB assay as described previously.<sup>67</sup> Briefly, cells were seeded at appropriate densities (4000 cells/well for MCF7 and WI38 and 2000 cells/well for A549) into the wells of 96-well plates in their corresponding medium and incubated overnight to allow the cells to attach. Subsequently, cells were exposed to freshly made solutions of drugs (ranging from 0.1 to 50  $\mu$ M) and incubated for a further 96 h. At the end of the incubation period, the medium was removed and cells were fixed with ice-cold trichloroacetic acid (TCA) (10%, w/v) for 30 min. Following extensive washing, the cells were stained with 0.4%

SRB dissolved in 1% acetic acid for 15 min at room temperature. The IC<sub>50</sub> value, the concentration required to inhibit cell growth by 50%, was determined from the mean absorbance at 540 nm for each drug concentration expressed as a percentage of the control untreated well absorbance.

**Immunoblotting.** MCF7 cells (5  $\times$  10<sup>6</sup> cells) were seeded in T75 cm<sup>2</sup> tissue culture flask with 10 mL of DMEM and treated with varying concentrations of test compounds for 24 h. At the end of the incubation period, cells were harvested by trypsinization followed by 1 $\times$  wash in PBS. The pellets were lysed using RIPA lysis buffer (Santa Cruz) on ice for 30 min. Lysates were spun at 14 000 rpm at 4 °C for 30 min, and protein samples were aliquoted and frozen at -80 °C. Total protein was quantified using BCA assay.

A 50  $\mu$ g amount of total protein from each sample was denatured in an equal volume of Laemmli buffer at 95 °C for 5 min. The samples were resolved on a 12% Tris-HCl SDS PAGE Precast gel (Biorad) followed by transfer to a 0.45  $\mu$ m pore size nitrocellulose membrane (Invitrogen, UK). The samples were probed with antibodies against histone, acetylated histone (Millipore), tubulin, acetylated tubulin (Sigma), p21 (Santa Cruz), and Actin (Abcam).

**Computational Methods.** The homology model of HDAC1 was calculated using SWISS-MODEL.<sup>68</sup> A set of 120 conformers of deprotonated 11c' was generated using MarvinSketch 5.1.5 (Chem-Axon Ltd.). Atomic charges were applied using ANTECHAMBER.<sup>69</sup> The conformers were extensively docked into the active site pocket of HDAC1 using DOCK6.4 and maximal 5000 orientations and 10 000 simplex iterations per conformer.<sup>70</sup> The ten conformers with the best scores were refined in a subsequent docking using AMBER scoring.<sup>71</sup> The best AMBER docking pose was used as a starting point for subsequent molecular dynamics calculations using GROMACS<sup>72</sup> and AMBER99<sup>73</sup> force fields. After in vacuo minimization using steepest-descent and conjugate-gradient algorithms, the complex consisting of HDAC1 and 11c' was solvated in a box containing 15526 TIP4 water molecules and 250 mM NaCl. A position-restrained dynamics simulation was run to equilibrate the water around the protein and to position water molecules and ligand within the active site of the enzyme. Then the temperature of the system was raised stepwise from 100 K to 300 K. In the last step at 300 K a period of 2 ns was simulated. The trajectory traces were analyzed using VMD 1.8.7 (University of Illinois).

## ■ ASSOCIATED CONTENT

### ● Supporting Information

NMR spectra for final compounds, NMR and MS data for the in situ reduction of 11c, selected dose-response curves for HDAC, DNMT1, and cell based assays, M.SssI data. This material is available free of charge via the Internet at <http://pubs.acs.org>.

## ■ AUTHOR INFORMATION

### Corresponding Author

\*Tel: (+44)20-75945815. Fax:(+44) 20-7594-5805. E-mail: m.fuchter@imperial.ac.uk.

### Notes

The authors declare no competing financial interest.

## ■ ACKNOWLEDGMENTS

This work was supported by the Association for International Cancer Research (AICR) (08-0407).

## ■ ABBREVIATIONS USED

CNS, central nervous system; DNMT, DNA methyltransferase; HAT, histone acetyltransferases; HDAC, histone deacetylase; NAD, nicotinamide adenine dinucleotide; SAH, S-adenosyl homocysteine; SAM, S-adenosyl methionine; TSA, trichostatin A

## ■ REFERENCES

- (1) Watt, F.; Molloy, P. L. Cytosine methylation prevents binding to DNA of a HeLa cell transcription factor required for optimal expression of the adenovirus major late promoter. *Genes Dev.* **1988**, *2*, 1136–1143.
- (2) Dong, A.; Yoder, J. A.; Zhang, X.; Zhou, L.; Bestor, T. H.; Cheng, X. Structure of human DNMT2, an enigmatic DNA methyltransferase homolog that displays denaturant-resistant binding to DNA. *Nucleic Acids Res.* **2001**, *29*, 439–448.
- (3) Okano, M.; Xie, S.; Li, E. Dnmt2 is not required for de novo and maintenance methylation of viral DNA in embryonic stem cells. *Nucleic Acids Res.* **1998**, *26*, 2536–2540.
- (4) Yoo, C. B.; Jones, P. A. Epigenetic therapy of cancer: past, present and future. *Nature Rev. Drug Discovery* **2006**, *5*, 37–50.
- (5) Chedin, F.; Lieber, M. R.; Hsieh, C. L. The DNA methyltransferase-like protein DNMT3L stimulates de novo methylation by Dnmt3a. *Proc. Natl. Acad. Sci. U.S.A.* **2002**, *99*, 16916–16921.
- (6) Chen, Z. X.; Mann, J. R.; Hsieh, C. L.; Riggs, A. D.; Chedin, F. J. Physical and functional interactions between the human DNMT3L protein and members of the de novo methyltransferase family. *Cell Biochem.* **2005**, *95*, 902–917.
- (7) Jia, D.; Jurkowska, R. Z.; Zang, X.; Jeltsch, A.; Cheng, X. Structure of Dnmt3a bound to Dnmt3L suggests a model for de novo DNA methylation. *Nature* **2007**, *449*, 248–251.
- (8) (a) Karet, M. S.; Botello, Z. M.; Ennis, J. J.; Chou, C.; Chedin, F. J. Reconstitution and mechanism of the stimulation of de novo methylation by human DNMT3L. *J. Biol. Chem.* **2006**, *281*, 25893–25902. (b) Bourc'his, D.; Xu, G. L.; Lin, C. S.; Bollman, B.; Bestor, T. H. Dnmt3L and the establishment of maternal genomic imprints. *Science* **2001**, *294*, 2536–2539.
- (9) Bourc'his, D.; Bestor, T. H. Meiotic catastrophe and retrotransposon reactivation in male germ cells lacking Dnmt3L. *Nature* **2004**, *431*, 96–99.
- (10) Ooi, S. K. e. a. DNMT3L connects unmethylated lysine 4 of histone H3 to de novo methylation of DNA. *Nature* **2007**, *448*, 714–717.
- (11) Johnstone, R. W. Histone Deacetylase inhibitors: novel drugs for the treatment of cancer. *Nature Rev. Drug Discovery* **2002**, *1*, 287–299.
- (12) Xu, W.; Parmigiani, R.; Marks, P. Histone deacetylase inhibitors: molecular mechanisms of action. *Oncogene* **2007**, *26*, 5541–5552.
- (13) Crabb, S.; Howell, M.; Rogers, H.; Ishfaq, M.; Yurek-George, A.; Carey, K.; Pickering, B.; East, P.; Mitter, R.; Maeda, S.; Johnson, P.; Townsend, P.; Shin-Ya, K.; Yoshida, M.; Ganesan, A.; Packham, G. Characterisation of the in vitro activity of the depsipeptide histone deacetylase inhibitor spiruchostatin A. *Biochem. Pharmacol.* **2008**, *76*, 463–475.
- (14) Miller, T.; Witter, D.; Belvedere, S. Histone deacetylase inhibitors. *J. Med. Chem.* **2003**, *46*, 5097–5116.
- (15) Biel, M.; Wascholowski, V.; Giannis, A. Epigenetics-An epicenter of gene regulation: histones and histone-modifying enzymes. *Angew. Chem., Int. Ed.* **2005**, *44*, 3186–3216.
- (16) Suzuki, T.; Miyata, N. Epigenetic control using natural products and synthetic molecules. *Curr. Med. Chem.* **2006**, *13*, 935–958.
- (17) Marks, P. A.; Breslow, R. Dimethyl sulfoxide to vorinostat: development of this histone deacetylase inhibitor as an anticancer drug. *Nat. Biotechnol.* **2007**, *25*, 84–90.
- (18) Mann, B. S.; Johnson, J. R.; Cohen, M. H.; Justice, R.; Pazdur, R. FDA approval summary: Vorinostat for treatment of advanced primary cutaneous T-cell lymphoma. *Oncologist* **2007**, *12*, 1247–1252.
- (19) Fang, M. Z.; Wang, Y.; Ai, N.; Hou, Z.; Sun, Y.; Lu, H.; Welsh, W.; Yang, C. S. Tea polyphenol (–)-epigallocatechin-3-gallate inhibits DNA methyltransferase and reactivates methylation-silenced genes in cancer cell lines. *Cancer Res.* **2003**, *63*, 7563–7570.
- (20) Lee, W. J.; Zhu, B. T. Inhibition of DNA methylation by caffeic acid and chlorogenic acid, two common catechol-containing coffee polyphenols. *Carcinogenesis* **2006**, *27*, 269–277.
- (21) Li, Y.; Liu, L.; Andrews, L. G.; Tollefsbol, T. O. Genistein depletes telomerase activity through cross-talk between genetic and epigenetic mechanisms. *Int. J. Cancer* **2009**, *125*, 286–296.
- (22) Pina, I. C.; Gautschi, J. T.; Wang, G. Y. S.; Sanders, M. L.; Schmitz, F. J.; France, D.; Cornell-Kennon, S.; Sambucetti, L. C.; Remiszewski, S. W.; Perez, L. B.; Bair, K. W.; Crews, P. Psammaplins from the sponge *Pseudoceratina purpurea*: inhibition of both histone deacetylase and DNA methyltransferase. *J. Org. Chem.* **2003**, *68*, 3866–3873.
- (23) Quinoa, E.; Crews, P. Phenolic constituents of Psammaplysilla. *Tetrahedron Lett.* **1987**, *28*, 3229–3232.
- (24) Arabshahi, L.; Schmitz, F. J. Brominated tyrosine metabolites from an unidentified sponge. *J. Org. Chem.* **1987**, *52*, 3584–3586.
- (25) Rodriguez, A. D.; Akee, R. K.; Scheuer, P. J. Two bromotyrosine-cysteine derived metabolites from a sponge. *Tetrahedron Lett.* **1987**, *28*, 4989–4992.
- (26) Kim, D.; Lee, I. S.; Jung, J. H.; Lee, C. O.; Choi, S. U. Psammaplin A, a natural phenolic compound, has inhibitory effect on human topoisomerase II and is cytotoxic to cancer cells. *Anticancer Res.* **1999**, *19*, 4085–4090.
- (27) Kim, D.; Lee, I. S.; Jung, J. H.; Yang, S. I. Psammaplin A, a natural bromotyrosine derivative from a sponge, possesses the antibacterial activity against methicillin-resistant *Staphylococcus aureus* and the DNA gyrase-inhibitory activity. *Arch. Pharm. Res.* **1999**, *22*, 25–29.
- (28) Shin, J.; Lee, H. S.; Seo, Y.; Rho, J. R.; Cho, K. W.; Paul, V. J. New bromotyrosine metabolites from the sponge *Aplysina rhax*. *Tetrahedron* **2000**, *56*, 9071–9077.
- (29) Tabudravu, J. N.; Eijssink, V. G. H.; Gooday, G. W.; Jaspars, M.; Komander, D.; Legg, M.; Synstad, B.; van Aalten, D. M. F. Psammaplin A, a chitinase inhibitor isolated from the Fijian marine sponge *Aplysina rhax*. *Bioorg. Med. Chem.* **2002**, *10*, 1123–1128.
- (30) Nicholas, G. M.; Eckman, L. L.; Ray, S.; Hughes, R. O.; Pfeifferkorn, J. A.; Barluenga, S.; Nicolaou, K. C.; Bewley, C. A. Bromotyrosine-derived natural and synthetic products as inhibitors of mycothiol-s-conjugate amidase. *Bioorg. Med. Chem. Lett.* **2002**, *12*, 2487–2490.
- (31) Shim, J. S.; Lee, H. S.; Shin, J.; Kwon, H. J. Psammaplin A, a marine natural product, inhibits aminopeptidase N and suppresses angiogenesis in vitro. *Cancer Lett.* **2004**, *203*, 163–169.
- (32) Jiang, Y.; Ahn, E.-Y.; Ryu, S. H.; Kim, D.-K.; Park, J.-S.; Yoon, H. J.; Yoo, S.; Lee, B.-J.; Lee, D. S.; Jung, J. H. Cytotoxicity of psammaplin A from a two-sponge association may correlate with the inhibition of DNA replication. *BMC Cancer* **2004**, *4*, doi:10.1186/1471-2407-4-70
- (33) (a) Park, Y.; Liu, Y.; Hong, J.; Lee, C.-O.; Cho, H.; Kim, D.-K.; Im, K. S.; Jung, J. H. New bromotyrosine derivatives from an association of two sponges, *Jaspis wondoensis* and *Poecillastra wondoensis*. *J. Nat. Prod.* **2003**, *66*, 1495–1498. (b) Nebbioso, A.; Pereira, R.; Khanwalkar, H.; Matarese, F.; Garcia-Rodriguez, J.; Miceli, M.; Logie, C.; Keding, V.; Ferrara, F.; Stunnenberg, H. G.; De Lera, A. R.; Gronemeyer, H.; Altucci, L. Death receptor pathway activation and increase of ROS production by the triple epigenetic inhibitor, UVI5008. *Mol. Cancer Ther.* **2011**, *10*, 2394–2404.
- (34) Kim, D. H.; Shin, J.; Kwon, H. J. Psammaplin A is a natural prodrug that inhibits class I histone deacetylase. *Exp. Mol. Med.* **2007**, *39*, 47–55.
- (35) Garcia, J.; Franci, G.; Pereira, R.; Benedetti, R.; Nebbioso, A.; Rodriguez-Barrios, F.; Gronemeyer, H.; Altucci, L.; de Lera, A. R. Epigenetic profiling of the antitumor natural product psammaplin A and its analogues. *Bioorg. Med. Chem.* **2011**, *19*, 3637–3649.
- (36) Baud, M. G. J.; Leiser, T.; Meyer-Almes, F.-J.; Fuchter, M. J. New synthetic strategies towards Psammaplin A, access to natural product analogues for biological evaluation. *Org. Biomol. Chem.* **2011**, *9*, 659–662.
- (37) Martin, N. L.; Woodward, J. J.; Marletta, M. A. N<sup>G</sup>-Hydroxyguanidines from primary amines. *Org. Lett.* **2006**, *8*, 4035–4038.
- (38) Siverstein, R. M.; Bassler, G. C.; Morill, T. C. *Spectrometric Identification of Organic Compounds*, 4th ed.; Wiley: New York, 1981.

- (39) Kazlauskas, R.; Lidgard, R. O.; Murphy, P. T.; Wells, R. J.; Blount, J. F. Brominated tyrosine-derived metabolites from the sponge *Ianthella basta*. *Aust. J. Chem.* **1981**, *34*, 765–786.
- (40) Yang, Q.; Liu, D.; Sun, D.; Yang, S.; Hu, G.; Wu, Z.; Zhao, L. Synthesis of the marine bromotyrosine psammaphin F and crystal structure of a psammaphin A Analogue. *Molecules* **2010**, *15*, 8784–8795.
- (41) Wang, D.; Helquist, P.; O., W. Zinc binding in HDAC inhibitors: A DFT study. *J. Org. Chem.* **2007**, *72*, 5446–5449.
- (42) Guénin, E.; M., M.; Bouchemal, N.; Prangé, T.; Lecouvey, M. Syntheses of phosphonic esters of alendronate, pamidronate and neridronate. *Eur. J. Org. Chem.* **2007**, 3380–3391.
- (43) Wegener, D.; Wirsching, F.; Riester, D.; Schwienhorst, A. A fluorogenic histone deacetylase assay well suited for high-throughput activity screening. *Chem. Biol.* **2003**, *10*, 61–68.
- (44) Hildmann, C.; Ninkovic, M.; Dietrich, R.; Wegener, D.; Riester, D.; Zimmermann, T.; Birch, O. M.; Bernegger, C.; Loidl, P.; Schwienhorst, A. A new amidohydrolase from *Bordetella* or *Alcaligenes* Strain FB188 with similarities to histone deacetylases. *J. Bacteriol.* **2004**, *186*, 2328–2339.
- (45) Nielsen, T. K.; Hildmann, C.; Dickmanns, A.; Schwienhorst, A.; Ficner, R. Crystal structure of a bacterial class 2 histone deacetylase homologue. *J. Mol. Biol.* **2005**, *354*, 107–120.
- (46) Jones, P.; Altamura, S.; Chakravarty, P. K.; Cecchetti, O.; De Francesco, R.; Gallinari, P.; Ingenito, R.; Meinke, P. T.; Petrocchi, A.; Rowley, M.; Scarpelli, R.; Serafini, S.; Steinkuhler, C. A series of novel, potent, and selective histone deacetylase inhibitors. *Bioorg. Med. Chem. Lett.* **2006**, *16*, 5948–5952.
- (47) (a) Suzuki, T.; Miyata, N. Non-hydroxamate Histone Deacetylase inhibitors. *Curr. Med. Chem.* **2005**, *12*, 2867–2880. (b) Wong, J. C.; Hong, R.; Schreiber, S. L. Structural biasing elements for in-cell Histone Deacetylase paralog selectivity. *J. Am. Chem. Soc.* **2003**, *125*, 5586–5587.
- (48) Bressi, J. C.; Jennings, A. J.; Skene, R.; Wu, Y.; Melkus, R.; De Jong, R.; O'Connell, S.; Grimshaw, C. E.; Navre, M.; Gangloff, A. R. Exploration of the HDAC2 foot pocket: Synthesis and SAR of substituted N-(2-aminophenyl)benzamides. *Bioorg. Chem. Med. Chem. Lett.* **2010**, *20*, 3142–3145.
- (49) Saavedra, O. M.; Isakovic, L.; Llewellyn, D. B.; Zhan, L.; Bernstein, N.; Claridge, S.; Raepel, F.; Vaisburg, A.; Elowe, N.; Petschner, A. J.; Rahil, J.; Beaulieu, N.; MacLeod, A. R.; Delorme, D.; Besterman, J. M.; Wahhab, A. SAR around (L)-S-adenosyl-L-homocysteine, an inhibitor of human DNA methyltransferase (DNMT) enzymes. *Bioorg. Chem. Med. Chem. Lett.* **2009**, *19*, 2747–2751.
- (50) Kuck, D.; Singh, N.; Lyko, F.; Medina-Franco, J. L. Novel and selective DNA methyltransferase inhibitors: Docking-based virtual screening and experimental evaluation. *Bioorg. Med. Chem.* **2010**, *18*, 822–829.
- (51) Posfai, J.; Bhagwat, A. S.; Posfai, G.; Roberts, R. J. Predictive motifs derived from cytosine methyltransferases. *Nucleic Acids Res.* **1989**, *17*, 2421–2435.
- (52) Takiguchi, M.; Achanzar, W. E.; Qu, W.; Guying, L.; Waalkes, M. P. Effects of cadmium on DNA-(cytosine-5) methyltransferase activity and DNA methylation status during cadmium-induced cellular transformation. *Exp. Cell Res.* **2003**, *286*, 355–365.
- (53) Godert, A. M.; Angelino, N.; Woloszynska-Read, A.; Morey, S. R.; James, S. R.; Karpf, A. R.; Sufirin, J. R. An improved synthesis of psammaphin A. *Bioorg. Med. Chem. Lett.* **2006**, *16*, 3330–3333.
- (54) Alao, J. P.; Stavropoulou, A. V.; Lam, E. W.-F.; Coombes, R. C.; Vigushin, D. M., Histone deacetylase inhibitor, Trichostatin A induces ubiquitin-dependent cyclin D1 degradation in MCF-7 breast cancer cells. *Mol. Cancer* **2006**, *5*, doi:10.1186/1476-4598-5-8.
- (55) Huang, L.; Sowa, Y.; Sakai, T.; Pardee, A. B. Activation of the p21WAF1/CIP1 promoter independent of p53 by the histone deacetylase inhibitor suberoylanilide hydroxamic acid (SAHA) through the Sp1 sites. *Oncogene* **2000**, *19*, 5712–5719.
- (56) Furumai, R.; Matsuyama, A.; Kobashi, N.; Lee, K.-H.; Nishiyama, M.; Nakajima, H.; Tanaka, A.; Komatsu, Y.; Nishino, N.; Yoshida, M.; Horinouchi, S. FK228 (Depsipeptide) as a natural prodrug that inhibits class I histone deacetylases. *Cancer Res.* **2002**, *62*, 4916–4921.
- (57) (a) Suzuki, T.; Nagano, Y.; Matsuura, A.; Kohara, A.; Ninomiya, S.; Kohda, K.; Miyata, N. Novel histone deacetylase inhibitors: design, synthesis, enzyme inhibition, and binding mode study of SAHA-Based non-hydroxamates. *Bioorg. Med. Chem. Lett.* **2003**, *13*, 4321–4326. (b) Suzuki, T.; Kouketsu, A.; Matsuura, A.; Kohara, A.; Ninomiya, S.; Kohda, K.; Miyata, N. Thiol-based SAHA analogues as potent histone deacetylase inhibitors. *Bioorg. Med. Chem. Lett.* **2004**, *14*, 3313–3317. (c) Suzuki, T.; Matsuura, A.; Kouketsu, A.; Hisakawa, S.; Nakagawa, H.; Miyata, N. Design and synthesis of non-hydroxamate histone deacetylase inhibitors: identification of a selective histone acetylating agent. *Bioorg. Med. Chem.* **2005**, *13*, 4332–4342. (d) Suzuki, T.; Matsuura, A.; Kouketsu, A.; Nakagawa, H.; Miyata, N. Identification of a potent non-hydroxamate histone deacetylase inhibitor by mechanism-based drug design. *Bioorg. Med. Chem. Lett.* **2005**, *15*, 331–335. (e) Suzuki, T.; Nagano, Y.; Kouketsu, A.; Matsuura, A.; Maruyama, S.; Kurotaki, M.; Nakagawa, H.; Miyata, N. Novel inhibitors of human histone deacetylases: design, synthesis, enzyme inhibition, and cancer cell growth inhibition of SAHA-based non-hydroxamates. *J. Med. Chem.* **2005**, *48*, 1019–1032.
- (58) Finnin, M. S.; Donigian, J. R.; Cohen, A.; Richon, V. M.; Rifkind, R. A.; Marks, P. A.; Breslow, R.; Pavletich, N. P. Structures of a histone deacetylase homologue bound to the TSA and SAHA inhibitors. *Nature* **1999**, *401*, 188–193.
- (59) Ficner, R. Novel structural insights into class I and II histone deacetylases. *Curr. Top. Med. Chem.* **2009**, *9*, 235–240.
- (60) Karpf, A. R.; Lasek, A. W.; Ririe, T. O.; Hanks, A. N.; Grossman, D.; Jones, D. A. Limited gene activation in tumor and normal epithelial cells treated with the DNA methyltransferase inhibitor 5-aza-2'-deoxycytidine. *Mol. Pharmacol.* **2004**, *65*, 18–27.
- (61) Remiszewski, S. W. The discovery of NVP-LAQ824: from concept to clinic. *Curr. Med. Chem.* **2003**, *10*, 2393–2402.
- (62) Ahn, M. Y.; Jung, J. H.; Na, Y. J.; Kim, H. S. A natural histone deacetylase inhibitor, Psammaphin A, induces cell cycle arrest and apoptosis in human endometrial cancer cells. *Gynecol. Oncol.* **2008**, *108*, 27–33.
- (63) Zhu, Y.; Wei, Q.; Lu, Y.; Yao, J.; Cao, X. Inhibition of proliferation induced by anti-sense RNA of HDAC1 in MCF-7 cells. *Mol. Med. Rep.* **2009**, *2*, 743–747.
- (64) Munster, P. N.; Thurn, K. T.; Thomas, S.; Raha, P.; Lacevic, M.; Miller, A.; Melisko, M.; Ismail-Khan, R.; Hugo, H.; Moasser, M.; Minton, S. E. A phase II study of the histone deacetylase inhibitor vorinostat combined with tamoxifen for the treatment of patients with hormone therapy-resistant breast cancer. *Br. J. Cancer* **2011**, *104*, 1828–1835.
- (65) Amundsen, A. R.; Whelan, J.; Bosnich, B. Biological analogues. On the nature of the binding sites of copper-containing proteins. *J. Am. Chem. Soc.* **1977**, *99*, 6730–6739.
- (66) Volund, A. Application of the four-parameter logistic model to bioassay: comparison with slope ratio and parallel line models. *Biometrics* **1978**, *34*, 357–365.
- (67) Skehan, P.; Storeng, R.; Scudiero, D.; Monks, A.; McMahon, J.; Vistica, D.; Warren, J. T.; Bokesch, H.; Kenney, S.; Boyd, M. R. New colorimetric cytotoxicity assay for anticancer-drug screening. *J. Natl. Cancer Inst.* **1990**, *82*, 1107–1112.
- (68) Arnold, K.; Bordoli, L.; Kopp, J.; T., S. The Swiss-Model workspace: a web-based environment for protein structure homology modelling. *Bioinformatics* **2006**, *22*, 195–201.
- (69) Wang, J.; Wang, W.; Kollman, P. A.; Case, D. A. Automatic atom type and bond type perception in molecular mechanical calculations. *J. Mol. Graphics Model.* **2006**, *25*, 247–260.
- (70) Lang, P. T.; Brozell, S. R.; Mukherjee, S.; Pettersen, E. F.; Meng, E. C.; Thomas, V.; Rizzo, R. C.; Case, D. A.; James, T. L.; Kuntz, I. D. DOCK 6: Combining techniques to model RNA–small molecule complexes. *RNA* **2009**, *15*, 1219–1230.
- (71) Graves, A. P.; Shivakumar, D. M.; Boyce, S. E.; Jacobson, M. P.; Case, D. A.; Shoichet. Rescoring docking hit lists for model cavity

sites: predictions and experimental testing. *J. Mol. Biol.* **2008**, *377*, 914–934.

(72) Hess, B.; Kutzner, C.; Van der Spoel, D.; Lindahl, E. GROMACS 4: algorithms for highly efficient, load-balanced, and scalable molecular simulation. *J. Chem. Theory Comput.* **2008**, *4*, 435–447.

(73) Sorin, E. J.; Pande, V. S. Exploring the helix-coil transition via all-atom equilibrium ensemble simulations. *Biophys. J.* **2005**, *88*, 2472–2493.